

The Graph Limit of The Minimizer of The Onsager-Machlup Functional and Its Computation

Qiang Du¹, Tiejun Li^{2,*}, Xiaoguang Li³ & Weiqing Ren⁴

¹*Department of Applied Physics and Applied Mathematics, Columbia University, New York, NY 10027, USA;*

²*LMAM and School of Mathematical Sciences, Peking University, Beijing 100871, P.R.China;*

³*Beijing Computational Science Research Center, Beijing, 100193, China,*

MOE-LCSM, School of Mathematics and Statistics, Hunan Normal University, Changsha, Hunan 410081, P. R. China;

⁴*Department of Mathematics, National University of Singapore, Singapore 119076, Singapore*

Email: qd2125@columbia.edu, tieli@pku.edu.cn, lixiaoguang@hunnu.edu.cn, matrw@nus.edu.sg

Received January 1, 2017; accepted January 1, 2017

Abstract The Onsager-Machlup (OM) functional is well-known for characterizing the most probable transition path of a diffusion process with non-vanishing noise. However, it suffers from a notorious issue that the functional is unbounded below when the specified transition time T goes to infinity. This hinders the interpretation of the results obtained by minimizing the OM functional. We provide a new perspective on this issue. Under mild conditions, we show that although the infimum of the OM functional becomes unbounded when T goes to infinity, the sequence of minimizers does contain convergent subsequences on the space of curves. The graph limit of this minimizing subsequence is an extremal of the abbreviated action functional, which is related to the OM functional via the Maupertuis principle with an optimal energy. We further propose an energy-climbing geometric minimization algorithm (EGMA) which identifies the optimal energy and the graph limit of the transition path simultaneously. This algorithm is successfully applied to several typical examples in rare event studies. Some interesting comparisons with the Freidlin-Wentzell action functional are also made.

Keywords Onsager-Machlup functional, Freidlin-Wentzell functional, graph limit, geometric minimization, Maupertuis principle

MSC(2010) 14Axx, 32Bxx

Citation: Qiang Du, Tiejun Li, Xiaoguang Li, Weiqing Ren. The Graph Limit of The Minimizer of The Onsager-Machlup Functional and Its Computation. *Sci China Math*, 2017, 60, doi: 10.1007/s11425-000-0000-0

1 Introduction

Consider a stochastic dynamics modeled by the stochastic differential equation (SDE)

$$d\mathbf{X}_t = \mathbf{b}(\mathbf{X}_t) dt + \sqrt{2\varepsilon} d\mathbf{W}_t, \quad (1.1)$$

where $\mathbf{X}_t, \mathbf{b} \in \mathbb{R}^d$, $\mathbf{W}_t = (W_t^1, W_t^2, \dots, W_t^d)$ is the standard d -dimensional Wiener process with $\mathbb{E}W_t^i = 0$ and $\mathbb{E}(W_t^i W_s^j) = \delta_{ij} \cdot \min(t, s)$ for $i, j = 1, \dots, d$ and $t, s \in \mathbb{R}^+$. Due to the presence of the noise, the system makes transitions from one metastable state to another; when ε is small, however, these transitions

* Corresponding author

happen on a time scale which is much longer than the relaxation time scale of the system. These rare but important transition events are very common in different fields of science, and their study has attracted much attention in recent years [2–4, 14, 21, 32]. One major object in the study of such rare events is to understand the transition mechanism, which can be characterized by the most probable path (MPP), i.e. the transition path with a dominant probability, connecting an initial state \mathbf{x}_s and a terminal state \mathbf{x}_f in the configuration space. How to characterize and compute these transition paths is a fundamental problem in the study of rare events [9, 10, 13, 22, 30, 34, 37, 40] and also the focus of this paper. In particular, we study the transition path at finite noise provided by the Onsager-Machlup functional and its graph limit as the prescribed transition time goes to infinity.

In the zero noise limit, i.e. $\varepsilon \rightarrow 0$, it is well-known from the large deviation theory that the MPP from \mathbf{x}_s to \mathbf{x}_f is given by the solution to the double minimization problem [11, 22]

$$S^{\text{FW}}(\mathbf{x}_s, \mathbf{x}_f) = \inf_{T>0} \inf_{\psi(0)=\mathbf{x}_s, \psi(T)=\mathbf{x}_f} S_T^{\text{FW}}[\psi], \quad (1.2)$$

where $\psi(t)$ is an absolutely continuous function on $[0, T]$ and $S_T^{\text{FW}}[\psi]$ is the Freidlin-Wentzell (FW) action functional

$$S_T^{\text{FW}}[\psi] = \int_0^T \frac{1}{2} |\dot{\psi} - \mathbf{b}(\psi)|^2 dt. \quad (1.3)$$

Here $\dot{\psi}$ denotes the time derivative of ψ . It is known that the infimum is achieved when $T = \infty$ if the MPP connecting \mathbf{x}_s and \mathbf{x}_f passes through a stationary point of the deterministic dynamics $\dot{\mathbf{x}} = \mathbf{b}(\mathbf{x})$. The quasi-potential $S^{\text{FW}}(\mathbf{x}_s, \mathbf{x}_f) = \inf_T \inf_{\psi} S_T^{\text{FW}}[\psi]$ characterizes, in the zero-noise limit, the transition rate, the invariant distribution of the stochastic dynamics and so forth. To avoid the difficulty caused by the infinite transition time, an alternative approach, which uses the arclength parameterization, has been proposed for the computation of the MPP on the space of curves [22].

For finite $\varepsilon > 0$, the Onsager-Machlup (OM) functional has been proposed in the literature to find the MPP [8, 16, 17, 25, 30, 35]. The OM functional is given by

$$S_T^{\text{OM}}[\psi] = \int_0^T L(\psi, \dot{\psi}) dt \quad (1.4)$$

if ψ is absolutely continuous on $[0, T]$, and takes the infinite value otherwise. Here the OM Lagrangian is given by

$$L(\mathbf{x}, \mathbf{y}) = \frac{1}{2} |\mathbf{y} - \mathbf{b}(\mathbf{x})|^2 + \varepsilon \nabla \cdot \mathbf{b}(\mathbf{x}) = \frac{1}{2} |\mathbf{y}|^2 - \mathbf{b}(\mathbf{x}) \cdot \mathbf{y} - U(\mathbf{x}), \quad (1.5)$$

where $U(\mathbf{x})$, the so-called path potential [30], is given by

$$U(\mathbf{x}) = -\varepsilon \nabla \cdot \mathbf{b}(\mathbf{x}) - \frac{1}{2} |\mathbf{b}(\mathbf{x})|^2. \quad (1.6)$$

The OM functional was first introduced by Onsager and Machlup for SDEs with linear drift $\mathbf{b}(\mathbf{x}) = -\gamma \mathbf{x}$ and constant diffusion by means of path integrals [29]. Indeed, their original formulation does not contain the term $\varepsilon \nabla \cdot \mathbf{b}(\mathbf{x})$ in (1.5) as this is only a constant in the case of linear drift. It was later generalized to cases with nonlinear drift and non-constant diffusion terms based on either physical arguments [20] or more rigorous mathematical derivations [18, 23, 33, 36]. It was also argued in [9] that, in the scalar case with a constant diffusion, the MPP is given by the minimizer of the OM functional. Indeed, as shown in [18, 23, 33], the OM functional arises from the limiting probability of a δ -ball problem, i.e.

$$\mathbb{P} \left(\sup_{0 \leq t \leq T} |\mathbf{X}_t - \psi(t)| \leq \delta \right) \sim C \exp \left(-\frac{2\varepsilon \lambda T}{\delta^2} \right) \exp \left(-\frac{1}{2\varepsilon} S_T^{\text{OM}}[\psi] \right) \quad (1.7)$$

as $\delta \rightarrow 0+$. Here $\varepsilon > 0$ is fixed, C is a positive constant and λ is the leading eigenvalue of the operator $-\frac{1}{2}\Delta$ with zero boundary condition on the domain $|\mathbf{x}| \leq 1$. The first exponential term on the right hand side of (1.7) can be also identified as the probability $\mathbb{P}(\sup_{0 \leq t \leq T} |\sqrt{2\varepsilon} \mathbf{W}_t| \leq \delta)$. Equation (1.7) shows that the minimizer of the OM functional characterizes the MPP under a suitable rescaling as $\delta \rightarrow 0$ while

$\varepsilon > 0$ is fixed. This methodology has been used to find the MPP in many practical problems, such as in the study of transition pathways of phage- λ switching [35], conformation changes of polymer systems [16, 17], protein folding pathways [25], and the maximum posteriori estimator [8], etc.

Although both the FW and OM functionals are widely used in applications, the connection between them is not fully understood. In practice, making the choice between the FW and OM functionals is often still a dilemma. The minimization of the two functionals gives different results and the minimizer of the OM functional is even dependent on the choice of the transition time T . Understanding the relations between the FW and OM functionals is thus an interesting mathematical problem. One formal connection between these two is that the FW functional can be obtained from the OM functional by simply setting $\varepsilon = 0$, therefore, they are likely equivalent in the zero-noise limit under certain conditions. Another formal connection can be made via the path integral approach. With the Girsanov theorem, we have

$$\mathbb{E}F[\mathbf{X}_t] = \mathbb{E}\left(F[\mathbf{W}_t] \exp\left(-\frac{1}{2} \int_0^T |\mathbf{b}(\mathbf{W}_t)|^2 dt + \int_0^T \mathbf{b}(\mathbf{W}_t) d\mathbf{W}_t\right)\right) \quad (1.8)$$

for Brownian functional $F[\mathbf{X}]$, where we take $\varepsilon = 1/2$ for simplicity and \mathbf{X}_t is the solution of the SDE (1.1). In the path integral, we formally represent the Wiener measure using the density $p(\mathbf{x}) = Z^{-1} \exp\left(-\frac{1}{2} \int_0^T |\dot{\mathbf{x}}|^2 dt\right)$. Then the path weight for $\{\mathbf{X}_t\}_{t \in [0, T]}$ will be given by the exponential of the FW or OM functional respectively, depending on whether Ito or Stratonovich version of the stochastic integral $\int_0^T \mathbf{b}(\mathbf{W}_t) d\mathbf{W}_t$ being interpreted as $\int_0^T \mathbf{b}(\mathbf{x}) \cdot \dot{\mathbf{x}} dt$ in path integrals. There have been some investigations on the relationship between the FW and OM functionals. For example, in [31] it was shown that the OM functional Γ -converges to a functional completely characterized by the FW functional when $T = \varepsilon^{-1}$ and $\varepsilon \rightarrow 0$; in [30], the numerical studies showed that in general the OM functional does not have a lower bound as $T \rightarrow \infty$, and the minimizer of the OM functional with $\varepsilon > 0$ exhibits quite different behavior compared to that of the FW functional.

Accepting the assertion that the minimizer of OM functional characterizes the MPP for the SDEs (1.1) when ε is finite, in this paper, we analyze the behaviour of the minimizer as the prescribed transition time T goes to infinity. This is meaningful since the transition time between metastable states is usually exponentially large in $O(1/\varepsilon)$ as suggested by the Arrhenius law. In particular, we will focus on the graph limit of the OM minimizers on the space of curves. As we will show, the minimization problem with $T = \infty$ is not a well-posed problem. However, we can study the graph limit of the OM minimizers as T goes to infinity, and this graph limit indeed gives a simpler description about the MPP of the OM functional with finite but sufficiently large T . This fact is clearly demonstrated in the example shown in 2, in which the path with a sharp corner has a simpler structure but still well characterizes the transition path one would obtain with a sufficiently large T . In this sense, the graph limit can be viewed as a good description of the MPP of the OM functional when T is finite but sufficiently large. This situation draws an analogy with the shock solution of hyperbolic conservation laws where the discontinuous shock solution with vanishing viscosity provides a simpler description for the solution to the corresponding parabolic system with small viscosity [6].

A natural procedure to investigate this graph limit is to first find the minimizer with a fixed T , then let T go to infinity. However, this procedure based on the original OM functional is neither effective nor transparent for the characterization of the graph limit due to the time parametrization of the path. To avoid this difficulty, we directly study the limit of the minimizers on the space of curves in which the path is parametrized by the normalized arclength. This gives more direct physical intuition and indeed the time parameterization can be recovered from this geometric path afterwards. Specifically, using a similar idea employed in [22] we reformulate the double minimization problem in a geometric fashion and look for the extremal of the action functional

$$\hat{S}_E[\varphi] = \int_0^1 \sqrt{2E - 2U(\varphi)} |\varphi'| - \mathbf{b}(\varphi) \cdot \varphi' d\alpha \quad (1.9)$$

with a proper energy E , where $\varphi \in C[0, 1]$ is the geometric path with an arclength type of parameterization, and φ' is the derivative of φ with respect to $\alpha \in [0, 1]$ (see details in Theorems 3.9 and 3.10).

The functional $\hat{S}_E[\varphi]$ is referred to as the geometric OM functional. Numerically, this approach was also pursued in [15, 35], but no theory was developed there on the choice of the energy E beforehand. This point will be made clear in this work through rigorous analysis.

We now summarize the main contributions of this paper. First, we demonstrate that the cause of the singularity arising from minimizing $S_T^{\text{OM}}[\psi_T]$ when $T \rightarrow \infty$ can be explicitly identified by separating the OM functional into two parts: a regular part containing the geometric OM functional (1.9), and a singular part given by $-E(T)T$. It is this singular part that drives the OM functional to $-\infty$ as $T \rightarrow \infty$. The graph limit of the minimizer of the OM functional can be identified from the regular part, i.e. the geometric OM functional (1.9). This observation is crucial for the subsequent theoretical studies. Secondly, we prove that, up to a subsequence, the graph of the minimizer of the OM functional uniformly converges to φ^* as $T_k \rightarrow \infty$, and the corresponding transition energy E_k converges to $E^* = \max_{\mathbf{x}} U(\mathbf{x})$ for gradient dynamics with $\mathbf{b}(\mathbf{x}) = -\nabla V(\mathbf{x})$. Furthermore, we prove that the limit φ^* is an extremal of the geometric OM functional (1.9) with the energy $E = E^*$. Thirdly, we propose an iterative numerical method to identify the graph limit φ^* and at the same time, to compute the critical energy E^* . We also analyze the convergence of the semi-discretized numerical scheme and apply the numerical method to several typical model problems in rare event studies. On the technical side, proving the compactness of the graph minimizers is highly nontrivial and represents the main challenge in the analysis. To the best of our knowledge, both the theoretical results and the numerical method are new and should be beneficial to future studies in understanding FW-OM connections and calculus of variations with similar issues.

The rest of the paper is organized as follows. In Section 2, we introduce the notations and assumptions that are used in the later analysis. In Section 3, we theoretically study the graph limit of the minimizer of the OM functional by first transforming the minimization of the OM functional with respect to ψ and T into a geometric minimization problem on the space of curves through the Maupertuis principle. We then show the subsequence convergence of the graph minimizers and the convergence of the corresponding transition energy. In Section 4, we compare the minimizers of the FW and OM functionals for some simple but enlightening examples. In Section 5, we propose an iterative energy-climbing geometric minimization algorithm (EGMA) and discuss its convergence property. In Section 6, we apply the numerical method to some typical model problems and compare them with the FW minimizers. Some concluding remarks are made in Section 7. The technical details about the BV compactness of the derivative of $\{\varphi_k\}$, are provided in the Appendix.

2 Assumptions and preliminary setup

Before proceeding to the analysis of the OM functional, we first introduce some notations and assumptions. Our analysis will focus on gradient systems with the drift function $\mathbf{b}(\mathbf{x}) = -\nabla V(\mathbf{x})$ for some potential energy $V(\mathbf{x}) \in C^7(\mathbb{R}^d)$, although some results can be readily extended to the non-gradient case. In the special gradient flow case, the path potential $U(\mathbf{x})$, which plays an important role in the analysis of the OM functional, is given by

$$U(\mathbf{x}) = \varepsilon \Delta V(\mathbf{x}) - \frac{1}{2} |\nabla V(\mathbf{x})|^2. \quad (2.1)$$

We have $U(\mathbf{x}) \in C^5$ by the smoothness assumption on V . We further assume that the potentials V and U satisfy the following properties:

Assumption 2.1. *There exists a local minimizer \mathbf{x}_m of $V(\mathbf{x})$, such that $\nabla V(\mathbf{x}_m) = 0$, $\nabla^2 V(\mathbf{x}_m)$ is strictly positive definite.*

Assumption 2.2. *The maximum points of $U(\mathbf{x})$ are contained in a bounded domain.*

Assumption 2.3. *For any $E \in \mathbb{R}$, the level set $\mathcal{L}_E = \{\mathbf{x} \in \mathbb{R}^d | U(\mathbf{x}) = E\}$ can be decomposed into a finite number of closed and connected subsets, i.e.*

$$\mathcal{L}_E = \bigcup_{k=1}^N B_k, \quad (2.2)$$

where the subsets B_k are closed and connected, and $B_j \cap B_k = \emptyset$ if $j \neq k$.

When $\varepsilon = 0$, the path potential reduces to $U(\mathbf{x}) = -\frac{1}{2} |\nabla V|^2 \leq 0$, which attains its maximum iff $\nabla V(\mathbf{x}) = 0$, i.e. the stationary states of the deterministic dynamics $\dot{\mathbf{x}} = -\nabla V(\mathbf{x})$. Assumption 2.2 requires that all points satisfying $\nabla V(\mathbf{x}) = 0$ lie in a bounded region. This is a usual assumption when dealing with the FW functional. When ε is finite but not very large, this requirement is not restrictive either. Indeed this is true in most previous studies on the OM functional.

For the FW functional, the point \mathbf{x}^* is called a critical point if $\nabla V(\mathbf{x}^*) = 0$. In the following, we generalize this concept to the OM functional.

Definition 2.4. $\mathbf{x}^* \in \mathbb{R}^d$ is called a critical point of the OM functional if

$$U(\mathbf{x}^*) = \max_{\mathbf{y} \in \mathbb{R}^d} U(\mathbf{y}). \tag{2.3}$$

Denoting the set of critical points by Λ , we make the following mild assumptions on them.

Assumption 2.5. Λ is discrete and has no accumulation points.

Assumption 2.6. $\nabla^2 U(\mathbf{x})$ has no zero eigenvalue for every $\mathbf{x} \in \Lambda$.

Let $C[0, T]$ denote the set of continuous functions on $[0, T]$ equipped with the norm $\|f\| = \sup_{t \in [0, T]} |f(t)|$. Define

$$C_{\mathbf{x}_s}^{\mathbf{x}_f}[0, T] = \{\psi \in C[0, T] \mid \psi(0) = \mathbf{x}_s, \psi(T) = \mathbf{x}_f\}.$$

Moreover, let $\bar{C}[0, T]$, $\bar{C}_{\mathbf{x}_s}^{\mathbf{x}_f}[0, T]$ be the set of corresponding absolutely continuous functions. We further define

$$\bar{C}_M^{\mathbf{x}_s, \mathbf{x}_f}[0, T] = \{\psi \in \bar{C}_{\mathbf{x}_s}^{\mathbf{x}_f}[0, T] \mid |\dot{\psi}| \leq M \text{ a.e.}\} \tag{2.4}$$

and

$$\bar{C}_{M,E}^{\mathbf{x}_s, \mathbf{x}_f}[0, T] = \{\psi \in \bar{C}_M^{\mathbf{x}_s, \mathbf{x}_f}[0, T] \mid U(\psi(t)) \leq E, t \in [0, T]\} \tag{2.5}$$

for $M > 0$.

Lemma 2.7 (Compactness of \bar{C}_M and $\bar{C}_{M,E}$). (1) For any $M > 0$, $\mathbf{x}_s, \mathbf{x}_f \in \mathbb{R}^d$, the set $\bar{C}_M^{\mathbf{x}_s, \mathbf{x}_f}[0, T]$ is compact in $C[0, T]$.

(2) For any $M > 0, E \in \mathbb{R}$, $\mathbf{x}_s, \mathbf{x}_f \in \mathbb{R}^d$, the set $\bar{C}_{M,E}^{\mathbf{x}_s, \mathbf{x}_f}[0, T]$ is compact in $C[0, T]$.

Proof. The first statement is the same as Lemma 2.5 in [22], which is a standard application of Arzelà-Ascoli theorem. The second statement is true since U is continuous and $\bar{C}_{M,E}^{\mathbf{x}_s, \mathbf{x}_f}$ is a closed subset of $\bar{C}_M^{\mathbf{x}_s, \mathbf{x}_f}$. \square

Hereafter, we will neglect the super- or sub-scripts \mathbf{x}_s and \mathbf{x}_f to simplify the notations when we do not emphasize the dependence on the initial and terminal states. It is also evident that the function spaces defined above and the compactness lemma are also applicable to functions on the interval $[0, 1]$, which is the case when we study the geometric minimizer on the space of curves. With a slight abuse of notation, we will use \bar{C}_M ($\bar{C}_{M,E}$) for $\bar{C}_M[0, T]$ ($\bar{C}_{M,E}[0, T]$) or $\bar{C}_M[0, 1]$ ($\bar{C}_{M,E}[0, 1]$) in later text when the domain is not specifically emphasized.

For every function $f \in \bar{C}[0, T]$, we denote its graph by

$$\gamma(f) = \{f(t) \mid t \in [0, T]\}.$$

For any two functions $f_1 \in \bar{C}[0, T_1]$ and $f_2 \in \bar{C}[0, T_2]$ with possibly different parameterizations, we use the Fréchet distance to measure the distance between their graphs $\gamma(f_1)$ and $\gamma(f_2)$:

$$\rho(f_1, f_2) = \inf_{t_i: [0, 1] \rightarrow [0, T_i], i=1,2} \max_{\alpha \in [0, 1]} |f_1 \circ t_1(\alpha) - f_2 \circ t_2(\alpha)|, \tag{2.6}$$

where the infimum is taken over all monotonically increasing, continuous and surjective reparametrizations t_1 and t_2 . It is easy to check that $\rho(f_1, f_2) = 0$ if the two functions have the same graph.

Given the initial and final states $\mathbf{x}_s, \mathbf{x}_f$, we aim at solving the double minimization problem

$$\inf_{T>0} \inf_{\psi \in C_{\mathbf{x}_s, \mathbf{x}_f}^{0,T}} \left\{ S_T^{\text{OM}}[\psi] = \int_0^T \left(\frac{1}{2} |\dot{\psi} + \nabla V(\psi)|^2 - \varepsilon \Delta V(\psi) \right) dt \right\}. \quad (2.7)$$

Note that

$$\begin{aligned} S_T^{\text{OM}}[\psi] &= \int_0^T \left(\frac{1}{2} |\dot{\psi}|^2 + \nabla V \cdot \dot{\psi} - U(\psi) \right) dt \\ &= \int_0^T \left(\frac{1}{2} |\dot{\psi}|^2 - U(\psi) \right) dt + V(\mathbf{x}_f) - V(\mathbf{x}_s). \end{aligned}$$

Since $V(\mathbf{x}_f) - V(\mathbf{x}_s)$ is a constant when \mathbf{x}_s and \mathbf{x}_f are given, we will ignore this constant and use the resulting simplified functional in place of $S_T^{\text{OM}}[\psi]$. With a slight abuse of notation, we still use $S_T^{\text{OM}}[\psi]$ to denote the simplified functional and call it the OM functional:

$$S_T^{\text{OM}}[\psi] = \int_0^T L(\psi, \dot{\psi}) dt, \quad (2.8)$$

where the Lagrangian $L(\mathbf{x}, \mathbf{y})$ is given by

$$L(\mathbf{x}, \mathbf{y}) = \frac{1}{2} |\mathbf{y}|^2 - U(\mathbf{x}). \quad (2.9)$$

In the following, we assume that for any fixed $T > 0$, the minimizer of $S_T^{\text{OM}}[\psi]$ is unique and has a uniformly bounded finite length. We state it precisely as follows.

Assumption 2.8. For any given $\mathbf{x}_s, \mathbf{x}_f \in \mathbb{R}^d$ and $T > 0$, $S_T^{\text{OM}}[\psi]$ has a unique minimizer ψ_T .

Assumption 2.9. For any given $\mathbf{x}_s, \mathbf{x}_f \in \mathbb{R}^d$ and $T > 0$, there exists a constant $M = M(\mathbf{x}_s, \mathbf{x}_f) > 0$ such that the minimizer ψ_T of $S_T^{\text{OM}}[\psi]$ satisfies

$$\int_0^T |\dot{\psi}_T| dt \leq M.$$

Corollary 2.10. Under the Assumption 2.9, ψ_T is uniformly bounded in $C[0, T]$ for any $T > 0$.

Proof. We have

$$|\psi_T(t)| = \left| \psi_T(0) + \int_0^t \dot{\psi}_T(s) ds \right| \leq |\mathbf{x}_s| + \int_0^t |\dot{\psi}_T| ds \leq |\mathbf{x}_s| + M. \quad (2.10)$$

□

The boundedness of ψ_T also implies the boundedness of $f(\psi_T)$ for any continuous function f .

3 Graph limit of the OM minimizer

In this section, we study the minimizers of the OM functional and their graph limit. First, we consider the problem of minimizing the OM functional with the transition time T fixed. Then we transform the minimization problem to a geometric one in which the path is parameterized by the normalized arc-length using the Maupertuis principle. This is followed by the analysis of the minimization problem with respect to the transition time T . The last part of this section is concerned with the graph limit of the minimizers and its governing equation.

3.1 Minimizing $S_T^{\text{OM}}[\psi]$ for a fixed time T

We first consider the minimization of $S_T^{\text{OM}}[\psi]$ over the set of absolutely continuous functions connecting given initial and final states. For a fixed $T > 0$, this is a standard variational problem. The following proposition gives the regularity result of the minimizer and its governing equation.

Proposition 3.1. Assume that $V \in C^7(\mathbb{R}^d)$. For any $T > 0$, the functional $S_T^{\text{OM}}[\psi]$ is lower-semicontinuous in $\bar{C}_{\mathbf{x}_s}^{\mathbf{x}_f}[0, T]$, thus attains its minimum in $\bar{C}_M^{\mathbf{x}_s, \mathbf{x}_f}[0, T]$. Moreover, under the Assumption 2.9, the minimizer $\psi_T \in C^6[0, T]$ and satisfies the Euler-Lagrange equation

$$\mathcal{D}L = \frac{\partial L}{\partial \mathbf{x}}(\psi_T, \dot{\psi}_T) - \frac{d}{dt} \frac{\partial L}{\partial \mathbf{y}}(\psi_T, \dot{\psi}_T) = 0, \quad (3.1)$$

i.e.

$$\begin{cases} \ddot{\psi}_T + \nabla U(\psi_T) = 0, \\ \psi_T(0) = \mathbf{x}_s, \psi_T(T) = \mathbf{x}_f. \end{cases} \quad (3.2)$$

This proposition ensures the existence and smoothness of the minimizer in a proper function space. Its proof can be found in [19] (Proposition 4 in page 42).

Remark 3.2. For general systems with a drift $\mathbf{b}(\mathbf{x})$, the minimizer ψ_T satisfies the Euler-Lagrange equation

$$\ddot{\psi}_T + (\nabla \mathbf{b}^T - \nabla \mathbf{b}) \cdot \dot{\psi}_T + \nabla U(\psi_T) = 0, \quad (3.3)$$

where $(\nabla \mathbf{b})_{ij} = \partial b_i / \partial x_j$.

It is a classical result that the energy of the system is conserved along the path ψ_T , i.e.

$$\frac{1}{2} |\dot{\psi}_T|^2 + U(\psi_T) \equiv E, \quad \forall t \in [0, T]. \quad (3.4)$$

With the Assumption 2.8, the constant E is uniquely determined by the initial and terminal states $\mathbf{x}_s, \mathbf{x}_f$ and the transition time T . For fixed \mathbf{x}_s and \mathbf{x}_f , E is a function of T only. In this case, E and T are connected by the equation:

$$T = \int_{\gamma(\psi_T)} \frac{|d\psi_T|}{\sqrt{2K_{E(T)}(\psi_T)}}, \quad (3.5)$$

where $K_E(\psi) = E - U(\psi)$ is the kinetic energy, $\gamma(\psi_T)$ is the graph of ψ_T .

3.2 Maupertuis principle

In many cases, we are mainly interested in the graph of the transition path in the configuration space rather than how it is parameterized by time t . It is well known that the Maupertuis variational principle, which is equivalent to the Hamilton's variational principle, is more convenient for such representations [1, 24].

Theorem 3.3 (Maupertuis Principle). *Up to a reparameterization of the path, the minimizer of variational problem*

$$\inf_{\psi \in \bar{C}_{\mathbf{x}_s}^{\mathbf{x}_f}[0, T]} S_T^{\text{OM}}[\psi] \quad (3.6)$$

is an extremal of the functional

$$S_0[\psi] = \int_{\gamma(\psi)} \mathbf{p}(\psi, \dot{\psi}) \cdot d\psi \quad (3.7)$$

subject to the constraint $H(\psi, \mathbf{p}) \equiv E(T)$, where H is the corresponding Hamiltonian

$$H(\mathbf{x}, \mathbf{p}) = \frac{1}{2} |\mathbf{p}|^2 + U(\mathbf{x}), \quad (3.8)$$

and $\mathbf{p}(\psi, \dot{\psi}) = \frac{\partial L}{\partial \mathbf{y}}(\psi, \dot{\psi}) = \dot{\psi}$ is the momentum.

The functional $S_0[\psi]$ is called the abbreviated action functional or effective functional [24, 25, 35]. Note that the value of S_0 does not depend on how $\gamma(\psi)$ is parameterized. A convenient way is to parameterize it using the normalized arclength. The curve with this parameterization is denoted by $\varphi(\alpha)$, which is an element of $\bar{C}[0, 1]$, such that $\varphi(0) = \mathbf{x}_s$, $\varphi(1) = \mathbf{x}_f$ and $|\varphi'(\alpha)| \equiv \text{const}$ for $\alpha \in [0, 1]$. For the Hamiltonian

(3.8) under the constraint $H(\varphi, \mathbf{p}) \equiv E$ and using the normalized arclength parameterization for the curve, the abbreviated action functional becomes

$$\hat{S}_E[\varphi] = \begin{cases} \int_0^1 \sqrt{2K_E(\varphi)} |\varphi'| \, d\alpha, & \text{if } \varphi \in \bar{C}[0, 1], U(\varphi) \leq E \text{ for } \alpha \in [0, 1], \\ +\infty, & \text{otherwise.} \end{cases} \quad (3.9)$$

More specifically, suppose the minimizer of $S_T^{\text{OM}}[\psi]$ is ψ_T , we define the new parameter $\alpha = \ell(t)$ as

$$\ell(t) = \frac{1}{L} \int_0^t |\dot{\psi}_T(s)| \, ds, \quad \text{where } L = \int_0^T |\dot{\psi}_T| \, dt. \quad (3.10)$$

Let $\ell^{-1}(\alpha) = \inf\{t \in [0, T] | \ell(t) \geq \alpha\} \in [0, T]$, then by the Maupertuis principle,

$$\varphi_{E(T)}(\alpha) = \psi_T(\ell^{-1}(\alpha))$$

is an extremal of $\hat{S}_{E(T)}[\varphi]$. Note that $\dot{\ell}(t) = L^{-1}|\dot{\psi}_T|$ and $\psi_T \in C^2[0, T]$. We have that $\ell^{-1}(\alpha)$ is also twice differentiable when $|\dot{\psi}_T| \neq 0$ and

$$\left| \frac{d\varphi_E}{d\alpha} \right| = |\dot{\psi}_T| \frac{dt}{d\alpha} = L.$$

If ψ_T satisfies the Assumption 2.9, $\varphi_E \in \bar{C}_M[0, 1]$ with $M \geq L$. By the equation(3.4), $|\dot{\psi}_T| = 0$ iff $E(T) = U(\psi_T(t))$, so $\varphi_E(\alpha)$ is twice differentiable where $U(\varphi_E(\alpha)) < E$.

We emphasize that even when ψ_T is the minimizer of $S_T^{\text{OM}}[\psi]$, $\varphi_{E(T)}$ need not to be a minimizer of $\hat{S}_{E(T)}[\varphi]$ but only an extremal. An illustrative example will be discussed in Section 4.2.

Denote the Lagrangian of $\hat{S}_E[\varphi]$ by

$$L_E(\mathbf{x}, \mathbf{y}) = \sqrt{2K_E(\mathbf{x})} |\mathbf{y}|. \quad (3.11)$$

When $\mathbf{y} \neq 0$, $\partial L_E / \partial \mathbf{y}$ is well-defined. The extremal of $\hat{S}_E[\varphi]$, denoted by φ_E , satisfies the Euler-Lagrange equation in a weak form

$$\int_0^1 \frac{\partial L_E}{\partial \mathbf{y}} \cdot \Phi' \, d\alpha + \int_0^1 \frac{\partial L_E}{\partial \mathbf{x}} \cdot \Phi \, d\alpha = 0, \quad \forall \Phi \in C_0^\infty[0, 1]. \quad (3.12)$$

Using the specific form of L_E , we get

$$\int_0^1 \sqrt{2K_E(\varphi)} \frac{\varphi'}{|\varphi'|} \cdot \Phi' \, d\alpha - \int_0^1 \frac{|\varphi'| \nabla U(\varphi) \cdot \Phi}{\sqrt{2K_E(\varphi)}} \, d\alpha = 0. \quad (3.13)$$

When $U(\varphi_E) < E$, $\varphi_E \in C^2$, we have the strong form of the Euler-Lagrange equation

$$2K_E(\varphi)\varphi'' + |\varphi'|^2 (I - \hat{\tau} \otimes \hat{\tau}) \cdot \nabla U(\varphi) = 0, \quad \alpha \in (0, 1), \quad (3.14)$$

$$\varphi(0) = \mathbf{x}_s, \quad \varphi(1) = \mathbf{x}_f \quad \text{and} \quad (|\varphi'|)' = 0, \quad (3.15)$$

where $\hat{\tau} = \varphi' / |\varphi'|$ and $U(\varphi) < E$.

Moreover, Eq. (3.5) can be written as

$$T = \int_0^1 \frac{|\varphi'_{E(T)}|}{\sqrt{2K_{E(T)}(\varphi_{E(T)})}} \, d\alpha, \quad (3.16)$$

and the infimum of the OM functional $S_T^{\text{OM}}[\psi]$ is given by

$$\begin{aligned} S_T^{\text{OM}}[\psi_T] &= \int_0^T \left(\frac{1}{2} |\dot{\psi}_T|^2 - U(\psi_T) \right) \, dt \\ &= \int_0^T |\dot{\psi}_T|^2 \, dt - E(T)T \end{aligned}$$

$$\begin{aligned}
 &= \int_0^T \sqrt{2K_{E(T)}(\psi_T)} |\dot{\psi}_T| dt - E(T)T \\
 &= \hat{S}_{E(T)}[\varphi_{E(T)}] - E(T)T.
 \end{aligned} \tag{3.17}$$

The connection between $S_T^{\text{OM}}[\psi_T]$ and $\hat{S}_{E(T)}[\varphi_{E(T)}]$ in (3.17) is essential for later analysis.

Remark 3.4. The above results can be generalized to non-gradient systems. For a general system with a drift \mathbf{b} , we have the Lagrangian $L(\mathbf{x}, \mathbf{y}) = \frac{1}{2} |\mathbf{y}|^2 - \mathbf{b}(\mathbf{x}) \cdot \mathbf{y} - U(\mathbf{x})$ and the corresponding Hamiltonian $H(\mathbf{x}, \mathbf{p}) = \frac{1}{2} |\mathbf{p} + \mathbf{b}(\mathbf{x})|^2 + U(\mathbf{x})$. The Maupertuis principle also holds with the geometric functional

$$\hat{S}_E[\varphi] = \begin{cases} \int_0^1 (\sqrt{2K_E(\varphi)} |\varphi'| - \mathbf{b} \cdot \varphi') d\alpha, & \text{if } \varphi \in \bar{C}[0, 1] \text{ and } U(\varphi) \leq E, \\ +\infty, & \text{otherwise.} \end{cases} \tag{3.18}$$

With the Lagrangian $L_E(\mathbf{x}, \mathbf{y}) = \sqrt{2K_E(\mathbf{x})} |\mathbf{y}| - \mathbf{b}(\mathbf{x}) \cdot \mathbf{y}$, Eqs. (3.12), (3.16) and (3.17) still hold. The strong form of the Euler-Lagrange equation is

$$2K_E(\varphi)\varphi'' + \sqrt{2K_E(\varphi)}(\nabla \mathbf{b}^T - \nabla \mathbf{b})\varphi' + |\varphi'|^2 (I - \hat{\tau} \otimes \hat{\tau}) \cdot \nabla U(\varphi) = 0 \tag{3.19}$$

with the constraint $|\varphi'| = \text{const}$ and $U(\varphi) < E$.

3.3 Minimization when T goes to infinity

Given ψ_T , the minimizer of $S_T^{\text{OM}}[\psi]$, the value of $S_T^{\text{OM}}[\psi_T]$ can be viewed as a function of T . As we will see below, taking the limit of $S_T^{\text{OM}}[\psi_T]$ as $T \rightarrow \infty$ is equivalent to minimizing the OM functional with respect to ψ followed by the minimization with respect to $T > 0$. We will follow the double minimization approach, which provides insights to the numerical results obtained in [30] and also facilitates comparisons with FW functional. The double minimization problem (2.7) reduces to a minimization with respect to T : $S(\mathbf{x}_s, \mathbf{x}_f) = \inf_T S_T^{\text{OM}}[\psi_T]$. We have:

Proposition 3.5.

$$\frac{\partial \hat{S}_E[\varphi_E]}{\partial E} = T, \quad \frac{\partial S_T^{\text{OM}}[\psi_T]}{\partial T} = -E(T).$$

This is a classical result in the Hamilton-Jacobi theory. One may refer to [19] for a rigorous proof. A formal derivation is as follows.

$$\frac{\partial \hat{S}_E[\varphi_E]}{\partial E} = \int_0^1 \frac{|\varphi'_E| d\alpha}{\sqrt{2K_E(\varphi_E)}} + \int_0^1 \mathcal{D}L_E(\varphi_E, \varphi'_E) \frac{\partial \varphi_E}{\partial E} d\alpha. \tag{3.20}$$

Since φ_E is an extremal of $\hat{S}_{E(T)}[\varphi]$, we have $\mathcal{D}L_E(\varphi_E, \varphi'_E) = 0$, thus $\frac{\partial \hat{S}_E[\varphi_E]}{\partial E} = T$. Furthermore, by Eq. (3.17),

$$\frac{\partial S_T^{\text{OM}}[\psi_T]}{\partial T} = \frac{\partial \hat{S}_E[\varphi_E]}{\partial E} \frac{\partial E}{\partial T} - E(T) - T \frac{\partial E}{\partial T} = -E(T).$$

Next we show that $E(T) > 0$ when T is sufficiently large. Then it follows from Proposition 3.5 that $S_T^{\text{OM}}[\psi_T]$ is a decreasing function of T when T is sufficiently large.

Lemma 3.6.

$$\liminf_{T \rightarrow +\infty} E(T) \geq \max_{\mathbf{x} \in \mathbb{R}^d} U(\mathbf{x}) > 0.$$

Proof. By Assumption 2.1, we have $\max_{\mathbf{x} \in \mathbb{R}^d} U(\mathbf{x}) \geq U(\mathbf{x}_m) = \varepsilon \Delta V(\mathbf{x}_m) > 0$. Denote $E_m = \liminf_{T \rightarrow +\infty} E(T)$, $E_{\max} = \max_{\mathbf{x} \in \mathbb{R}^d} U(\mathbf{x})$, then there exists a sequence $T_k \rightarrow +\infty$ such that $E_k = E(T_k) \rightarrow E_m$.

We will prove the result by contradiction. If $\Delta E = E_{\max} - E_m > 0$, we have $E_{\max} - E_k > \frac{3}{4} \Delta E > 0$ when k is large enough. Denote the minimizer of $S_{T_k}^{\text{OM}}[\psi]$ by ψ_k , and the corresponding extremal of $\hat{S}_{E_k}[\varphi]$ that has the same graph as ψ_k by φ_k . We have

$$U(\varphi_k) \leq E_k < E_{\max} - \frac{3}{4} \Delta E$$

for any sufficiently large k . This implies that $\varphi_k(\alpha) \notin S = \{\mathbf{x} | E_{\max} - \Delta E/2 < U(\mathbf{x}) \leq E_{\max}\}$ for any $\alpha \in [0, 1]$. Let us choose a point \mathbf{x}_c from the set S . For T_k sufficiently large, let $\tilde{\psi}_1(t) \in \bar{C}_M^{\mathbf{x}_s, \mathbf{x}_c}[0, T_k/2]$ be the minimizer of $S_{T_k/2}^{\text{OM}}[\psi]$ with $\psi(0) = \mathbf{x}_s$, $\psi(T_k/2) = \mathbf{x}_c$. The energy conservation (3.4) yields

$$|\dot{\tilde{\psi}}_1|^2 + 2U(\tilde{\psi}_1) \equiv 2\tilde{E}_1$$

for some constant \tilde{E}_1 . Clearly, $\tilde{E}_1 \geq U(\mathbf{x}_c) > E_{\max} - \Delta E/2$. By the Maupertuis principle, there exists an extremal $\tilde{\varphi}_1 \in \bar{C}_M[0, 1]$ of $\hat{S}_{\tilde{E}_1}[\varphi]$ which has the same graph as $\tilde{\psi}_1$. Eq. (3.17) gives

$$S_{T_k/2}^{\text{OM}}[\tilde{\psi}_1] = \hat{S}_{\tilde{E}_1}[\tilde{\varphi}_1] - \frac{1}{2}\tilde{E}_1 T_k.$$

Similarly, let $\tilde{\psi}_2 \in \bar{C}_M^{\mathbf{x}_c, \mathbf{x}_f}[0, T_k/2]$ be the minimizer of $S_{T_k/2}^{\text{OM}}[\psi]$ with $\psi(0) = \mathbf{x}_c$ and $\psi(T_k/2) = \mathbf{x}_f$. The energy along $\tilde{\psi}_2$ satisfies $\tilde{E}_2 > E_{\max} - \Delta E/2$. Let $\tilde{\varphi}_2$ be the corresponding extremal of $\hat{S}_{\tilde{E}_2}[\varphi]$ which has the same graph as $\tilde{\psi}_2$. We have

$$S_{T_k/2}^{\text{OM}}[\tilde{\psi}_2] = \hat{S}_{\tilde{E}_2}[\tilde{\varphi}_2] - \frac{1}{2}\tilde{E}_2 T_k.$$

Define $\hat{\psi} \in \bar{C}_M[0, T_k]$ as

$$\hat{\psi}(t) = \begin{cases} \tilde{\psi}_1(t), & \text{if } 0 \leq t \leq \frac{1}{2}T_k, \\ \tilde{\psi}_2(t - \frac{1}{2}T_k), & \text{if } \frac{1}{2}T_k \leq t \leq T_k. \end{cases} \quad (3.21)$$

We have

$$\begin{aligned} S_{T_k}^{\text{OM}}[\hat{\psi}] - S_{T_k}^{\text{OM}}[\psi_k] &= \hat{S}_{\tilde{E}_1}[\tilde{\varphi}_1] + \hat{S}_{\tilde{E}_2}[\tilde{\varphi}_2] - \hat{S}_{E_k}[\varphi_k] - \frac{1}{2}(\tilde{E}_1 + \tilde{E}_2 - 2E_k)T_k \\ &\leq \int_0^1 \sqrt{2\tilde{E}_1 - 2U(\tilde{\varphi}_1)} |\tilde{\varphi}'_1| \, d\alpha + \int_0^1 \sqrt{2\tilde{E}_2 - 2U(\tilde{\varphi}_2)} |\tilde{\varphi}'_2| \, d\alpha \\ &\quad - \int_0^1 \sqrt{2E_k - 2U(\varphi_k)} |\varphi'_k| \, d\alpha - \frac{1}{4}\Delta E T_k. \end{aligned} \quad (3.22)$$

Since $\tilde{\varphi}_1, \tilde{\varphi}_2, \varphi_k \in \bar{C}_M[0, 1]$, $\hat{S}_{\tilde{E}_1}[\tilde{\varphi}_1]$, $\hat{S}_{\tilde{E}_2}[\tilde{\varphi}_2]$ and $\hat{S}_{E_k}[\varphi_k]$ are all uniformly bounded. Thus

$$S_{T_k}[\hat{\psi}] - S_{T_k}[\psi_k] \leq C - \frac{1}{4}\Delta E T_k < 0$$

when T_k is sufficiently large, where C is a generic constant. This contradicts with the assumption that ψ_k is the minimizer of $S_{T_k}[\psi]$. \square

Proposition 3.5 and Lemma 3.6 show that $S_T^{\text{OM}}[\psi_T]$ is a decreasing function of T with a positive decreasing rate when T is sufficiently large. Thus $S_T^{\text{OM}}[\psi_T] \rightarrow -\infty$ as $T \rightarrow +\infty$. Next we show that the infimum of $S_T^{\text{OM}}[\psi_T]$ occurs only when $T \rightarrow +\infty$.

Proposition 3.7. $S_T^{\text{OM}}[\psi_T]$ assumes its infimum only when $T \rightarrow +\infty$. Moreover, we have

$$\inf_{T>0} \inf_{\psi \in \bar{C}_{\mathbf{x}_s}^{\mathbf{x}_f}[0, T]} S_T^{\text{OM}}[\psi] = \lim_{T \rightarrow +\infty} \inf_{\psi \in \bar{C}_{\mathbf{x}_s}^{\mathbf{x}_f}[0, T]} S_T^{\text{OM}}[\psi] = -\infty.$$

Proof. By the mean value theorem and Assumption 2.9, we derive from Eq. (3.16) that

$$\frac{|\mathbf{x}_s - \mathbf{x}_f|}{\sqrt{2K_E(\psi_T(t_c))}} \leq T = \frac{\int_0^T |\dot{\psi}_T| \, dt}{\sqrt{2K_E(\psi_T(t_c))}} \leq \frac{M}{\sqrt{2K_E(\psi_T(t_c))}} \quad (3.23)$$

where $K_E(\psi_T(t_c)) = E(T) - U(\psi_T(t_c))$ for some $t_c \in [0, T]$. Thus

$$U(\psi_T(t_c)) + \frac{|\mathbf{x}_s - \mathbf{x}_f|^2}{2T^2} \leq E(T) \leq U(\psi_T(t_c)) + \frac{M^2}{2T^2}. \quad (3.24)$$

Since $\{\psi_T\}$ is uniformly bounded, $\{U(\psi_T)\}$ is also uniformly bounded by a constant M_U . Inequality (3.24) implies $E(T) \rightarrow +\infty$ when $T \rightarrow 0+$. By Proposition 3.5, $S_T^{\text{OM}}[\psi_T]$ is decreasing in a neighborhood of $T = 0$. So there exists $T_m > 0$, such that $S_T^{\text{OM}}[\psi_T]$ cannot attain its infimum in $T \in [0, T_m]$.

By Lemma 3.6, there exists $T_M > 0$ such that when $T > T_M$, $E(T) > \frac{1}{2}E_{\max} > 0$. For $T \in [T_m, T_M]$, (3.24) implies the uniform boundedness of $E(T)$. Denote the upper bound by M_E , lower bound m_E . For any path $\varphi \in \bar{C}_{M,E}[0, 1]$, φ is uniformly bounded. We have

$$\hat{S}_{E(T)}[\varphi_E] \leq M\sqrt{2M_E + 2M_U},$$

which yields

$$-M\sqrt{2M_E + M_U} - M_ET_m \leq S_T^{\text{OM}}[\psi_T] \leq M\sqrt{2M_E + M_U} - m_ET_M.$$

So $S_T^{\text{OM}}[\psi_T]$ is bounded in $[T_m, T_M]$.

When $T > T_M$, $S_T^{\text{OM}}[\psi_T]$ is a decreasing function of T . So

$$\inf_{T > T_M} \inf_{\psi} S_T^{\text{OM}}[\psi] = \lim_{T \rightarrow +\infty} \inf_{\psi} S_T^{\text{OM}}[\psi] \leq \lim_{T \rightarrow +\infty} M\sqrt{2M_E + 2M_U} - \frac{1}{2}E_{\max}T = -\infty.$$

Combining with previous facts we obtain

$$\inf_{T > 0} \inf_{\psi} S_T^{\text{OM}}[\psi] = \lim_{T \rightarrow +\infty} \inf_{\psi} S_T^{\text{OM}}[\psi] = -\infty.$$

□

Proposition 3.7 shows that the infimum of the OM functional is always negative infinity. This can be viewed as a special case of the so-called Mané potential [5, 28]. The Mané potential has a positive Mané critical value. This critical value is given by $E_{\max} = \max_{\mathbf{x} \in \mathbb{R}^d} U(\mathbf{x})$ for the OM functional. It can be shown that for any C below the critical value (e.g. $C = 0$ as in the current case), one has $\inf_T \inf_{\psi} S_T^{\text{OM}}[\psi] + CT = -\infty$. In this sense, we can also call $\hat{S}_E[\varphi]$ the *renormalized OM functional* since it removes the divergence term $-E(T)T$ as $T \rightarrow \infty$.

Remark 3.8. Propositions 3.5 and 3.7 can be generalized to non-gradient case with slight modifications.

3.4 The Graph limit of minimizers of OM functionals

Proposition 3.7 shows that it is inappropriate to define the minimizer (T^*, ψ_{T^*}) of the original functional $S_T^{\text{OM}}[\psi]$ with time parameterization. However, this limit process could be meaningful if we inspect the transition path sequence in the configuration space instead of using the time coordinate. Next we will study the graph limit of OM minimizers as $T \rightarrow +\infty$.

We have shown using the Maupertuis principle that for any $T > 0$, the minimizer ψ_T can be mapped to $\varphi \in C[0, 1]$ by a reparameterization such that $\gamma(\psi_T) = \gamma(\varphi)$. Moreover, φ is an extremal of $\hat{S}_E[\varphi]$ with $E = E(T)$. In the following, we show that there exist a proper energy parameter E^* , a path φ^* which is an extremal of $\hat{S}_{E^*}[\varphi]$ and a subsequence of the minimizer $\{\psi_{T_k}\}$, such that $\rho(\psi_{T_k}, \varphi^*) \rightarrow 0$ when $k \rightarrow \infty$.

Theorem 3.9. Let $\{T_k\}_{k=1}^{\infty}$ be a positive sequence such that $T_k \rightarrow +\infty$ when $k \rightarrow \infty$. Let ψ_k be the minimizer of the OM functional $S_{T_k}^{\text{OM}}[\psi]$, $E_k = E(T_k)$, and φ_k be the extremal of $\hat{S}_{E_k}[\varphi]$ which has the same graph as ψ_k . We have

- (1) There exists a subsequence $\{\varphi_{k_l}\}$ which uniformly converges to $\varphi^* \in \bar{C}_M^{\mathbf{x}_s, \mathbf{x}_f}[0, 1]$.
- (2) The subsequence $\{E_{k_l}\}$ converges to $E^* = \max_{\mathbf{x}} U(\mathbf{x})$ and $\varphi^* \in \bar{C}_{M, E^*}[0, 1]$.
- (3) φ^* passes through a critical point at some $\alpha_c \in [0, 1]$.
- (4) $\rho(\psi_{k_l}, \varphi^*) \rightarrow 0$ when $l \rightarrow +\infty$.

(5) For any $\delta > 0$, the integral

$$\int_{\alpha_c - \delta}^{\alpha_c + \delta} \frac{|\varphi^{*\prime}| \, d\alpha}{\sqrt{2E^* - 2U(\varphi^*)}}$$

diverges. In particular,

$$T^* = \int_0^1 \frac{|\varphi^{*\prime}| \, d\alpha}{\sqrt{2E^* - 2U(\varphi^*)}} = +\infty.$$

Proof. (1)-(2)-(3). Denote $U_k = \max_{\alpha} U(\varphi_k(\alpha))$. Eq. (3.16) gives

$$T_k = \int_0^1 \frac{|\varphi'_k| \, d\alpha}{\sqrt{2E_k - 2U(\varphi_k)}} \leq \frac{M}{\sqrt{2E_k - 2U_k}}. \quad (3.25)$$

So we have

$$U_k \leq E_k \leq U_k + \frac{M^2}{2T_k^2}. \quad (3.26)$$

By Assumption 2.9, $\{E_k\}$ is uniformly bounded by a constant M_E and $\varphi_k \in \bar{C}_{M, M_E}$. From Lemma 2.7, there exists a subsequence $\{k_l\}$ such that $E_{k_l} \rightarrow E^*$ and $\varphi_{k_l} \rightarrow \varphi^* \in \bar{C}_{M, M_E}$. To show $\varphi^* \in \bar{C}_{M, E^*}$, we note that

$$0 \leq E_{k_l} - U(\varphi_{k_l}) \rightarrow E^* - U(\varphi^*) \quad \text{when } l \rightarrow \infty,$$

which means $\max_{\alpha} U(\varphi^*(\alpha)) \leq E^*$.

Next we show $E^* = \max_{\alpha} U(\varphi^*(\alpha))$. Otherwise $E^* - \max_{\alpha \in [0, 1]} U(\varphi^*(\alpha)) = m > 0$. Since $E_{k_l} \rightarrow E^*$ and $\varphi_{k_l} \rightarrow \varphi^*$ uniformly, we have $|E_{k_l} - E^*| < \delta_0$, $|U(\varphi^*) - U(\varphi_{k_l})| < \delta_0$ for any positive δ_0 when l is sufficiently large. Choose $\delta_0 < m/4$, we obtain

$$E_{k_l} - U(\varphi_{k_l}) = (E_{k_l} - E^*) + (E^* - U(\varphi^*)) + (U(\varphi^*) - U(\varphi_{k_l})) > m - 2\delta_0 > 0. \quad (3.27)$$

Since $E_{k_l} - U(\varphi_{k_l}) \rightarrow E^* - U(\varphi^*)$, it follows from the dominate convergence theorem that

$$\begin{aligned} +\infty &= \lim_{l \rightarrow \infty} T_{k_l} = \lim_{l \rightarrow \infty} \int_0^1 \frac{|\varphi'_{k_l}| \, d\alpha}{\sqrt{2E_{k_l} - 2U(\varphi_k)}} \\ &\leq \lim_{l \rightarrow \infty} M \int_0^1 \frac{d\alpha}{\sqrt{2E_{k_l} - 2U(\varphi_k)}} = M \int_0^1 \lim_{l \rightarrow \infty} \frac{d\alpha}{\sqrt{2E_{k_l} - 2U(\varphi_k)}} \\ &\leq M \int_0^1 \frac{d\alpha}{\sqrt{2m}} = \frac{M}{\sqrt{2m}}, \end{aligned} \quad (3.28)$$

which is a contradiction. Thus $E^* = \max_{\alpha \in [0, 1]} U(\varphi^*(\alpha))$.

By Lemma 3.6, we have

$$\max_{\mathbf{x} \in \mathbb{R}^d} U(\mathbf{x}) \leq \liminf_{T \rightarrow +\infty} E(T) \leq E^* = \max_{\alpha \in [0, 1]} U(\varphi^*(\alpha)) \leq \max_{\mathbf{x} \in \mathbb{R}^d} U(\mathbf{x}).$$

So we have $E^* = \max_{\mathbf{x} \in \mathbb{R}^d} U(\mathbf{x}) = \max_{\alpha \in [0, 1]} U(\varphi^*(\alpha))$. It follows that there must exist an $\alpha_c \in [0, 1]$, such that $U(\varphi^*(\alpha_c)) = \max_{\mathbf{x} \in \mathbb{R}^d} U(\mathbf{x})$. Thus $\mathbf{x}_c = \varphi^*(\alpha_c)$ is a critical point.

(4). Since ψ_{k_l} has the same graph as φ_{k_l} , we have

$$\rho(\psi_{k_l}, \varphi^*) = \rho(\varphi_{k_l}, \varphi^*) \leq \max_{\alpha \in [0, 1]} |\varphi_{k_l}(\alpha) - \varphi^*(\alpha)| \rightarrow 0, \quad l \rightarrow +\infty.$$

(5). By Taylor expansion of $U(\varphi^*)$ near \mathbf{x}_c , we get

$$\begin{aligned} E^* - U(\varphi^*(\alpha)) &= -\frac{1}{2}[\varphi^*(\alpha) - \varphi^*(\alpha_c)]^T \nabla^2 U(\mathbf{x}_c) [\varphi^*(\alpha) - \varphi^*(\alpha_c)] \\ &\quad + o(|\varphi^*(\alpha) - \varphi^*(\alpha_c)|^2). \end{aligned} \quad (3.29)$$

By Assumption 2.6, we obtain

$$E^* - U(\varphi^*(\alpha)) \leq \frac{\mu_M}{2} |\varphi^*(\alpha) - \varphi^*(\alpha_c)|^2 + o(|\alpha - \alpha_c|)^2 \leq C |\alpha - \alpha_c|^2$$

for some constant $C > 0$ in a neighborhood of α_c , where μ_M is the largest eigenvalue of $-\nabla^2 U(\mathbf{x}_c)$. The integral

$$\int_{\alpha_c - \delta}^{\alpha_c + \delta} \frac{|\varphi^{*\prime}| \, d\alpha}{\sqrt{2E^* - 2U(\varphi^*)}} \geq \int_{\alpha_c - \delta}^{\alpha_c + \delta} \frac{|\mathbf{x}_s - \mathbf{x}_f| \, d\alpha}{\sqrt{2C} |\alpha - \alpha_c|} = +\infty.$$

This ends the proof of the last statement. \square

Theorem 3.9 shows that, up to a subsequence, the limiting transition energy E^* and the graph limit of the OM minimizer φ^* are well-defined. Next we show that the graph limit φ^* is an extremal of $\hat{S}_{E^*}[\varphi]$.

Theorem 3.10. *φ^* is an extremal of $\hat{S}_{E^*}[\varphi]$ passing through a critical point with $E^* = \max_{\mathbf{x} \in \mathbb{R}^d} U(\mathbf{x})$.*

The proof of Theorem 3.10 relies on the following result, whose proof is rather technical thus will be carried out in the Appendix.

Proposition 3.11. *There exists a subsequence $\{\varphi_{k_l}\}$ such that $\varphi'_{k_l} \rightarrow \varphi^{*\prime}$ almost everywhere.*

Proof of Theorem 3.10. By Theorem 3.9 and Proposition 3.11, there exists a subsequence $\{\varphi_{k_l}\}$ which satisfies (1) $\varphi_{k_l} \rightarrow \varphi^*$ uniformly; (2) $\varphi'_{k_l} \rightarrow \varphi^{*\prime}$ a.e.; (3) $E_{k_l} \rightarrow E^*$.

Since φ_{k_l} is an extremal of $\hat{S}_{E_{k_l}}[\varphi]$, it satisfies the Euler-Lagrange equation (3.13). We have

$$\lim_{l \rightarrow \infty} \int_0^1 \left(\sqrt{2K_{E_{k_l}}(\varphi_{k_l})} \frac{\varphi'_{k_l} \cdot \Phi'}{|\varphi'_{k_l}|} - \frac{|\varphi'_{k_l}| \nabla U(\varphi_{k_l}) \cdot \Phi}{\sqrt{2K_{E_{k_l}}(\varphi_{k_l})}} \right) d\alpha = 0, \quad \forall \Phi \in C_0^\infty[0, 1]. \quad (3.30)$$

From $\varphi_{k_l} \in \bar{C}_M[0, 1]$, we have $\sqrt{2K_{E_{k_l}}(\varphi_{k_l})} \leq M_1$ for some constant M_1 , thus

$$\sqrt{2K_{E_{k_l}}(\varphi_{k_l})} \frac{|\varphi'_{k_l} \cdot \Phi'|}{|\varphi'_{k_l}|} \leq M_1 |\Phi'|.$$

It follows from the dominated convergence theorem that

$$\lim_{l \rightarrow \infty} \int_0^1 \sqrt{2K_{E_{k_l}}(\varphi_{k_l})} \frac{\varphi'_{k_l} \cdot \Phi'}{|\varphi'_{k_l}|} d\alpha = \int_0^1 \sqrt{2K_{E^*}(\varphi^*)} \frac{\varphi^{*\prime} \cdot \Phi'}{|\varphi^{*\prime}|} d\alpha. \quad (3.31)$$

By Theorem 3.9, φ^* passes through a critical point \mathbf{x}_c at $\alpha = \alpha_c$. The Taylor expansion (3.29) shows

$$E^* - U(\varphi^*(\alpha)) \geq \frac{\mu_m}{2} |\varphi^*(\alpha) - \varphi^*(\alpha_c)|^2 + o(|\varphi^*(\alpha) - \varphi^*(\alpha_c)|^2),$$

where μ_m is the smallest eigenvalue of $-\nabla^2 U(\mathbf{x}_c)$. By Assumption 2.6, there is a constant $C_1 > 0$ such that $E^* - U(\varphi^*) \geq C_1 |\varphi^*(\alpha) - \varphi^*(\alpha_c)|^2$ in a neighborhood of α_c . Furthermore, we have

$$\begin{aligned} |\nabla U(\varphi^*)| &= |\nabla^2 U(\mathbf{x}_c)(\varphi^*(\alpha) - \varphi^*(\alpha_c))| + o(|\varphi^*(\alpha) - \varphi^*(\alpha_c)|) \\ &\leq \mu_M |\varphi^*(\alpha) - \varphi^*(\alpha_c)| + o(|\varphi^*(\alpha) - \varphi^*(\alpha_c)|). \end{aligned}$$

There exists a constant $C_2 > 0$ such that $|\nabla U(\varphi^*) \cdot \Phi| \leq C_2 |\Phi| |\varphi^*(\alpha) - \varphi^*(\alpha_c)|$. Combining the above results, we obtain

$$\frac{\nabla U(\varphi^*) \cdot \Phi}{\sqrt{2E^* - 2U(\varphi^*)}} \leq C |\Phi|,$$

where the right-hand side is a bounded function.

For any $l > 0$ and given $\Phi(\alpha)$, define

$$G_{k_l}(\alpha) = \frac{\nabla U(\varphi_{k_l}) \cdot \Phi}{\sqrt{2E_{k_l} - 2U(\varphi_{k_l})}} \quad \text{and} \quad G^*(\alpha) = \frac{\nabla U(\varphi^*) \cdot \Phi}{\sqrt{2E^* - 2U(\varphi^*)}}.$$

We know that $G_{k_l} \rightarrow G^*$ and G^* is bounded by a constant $C_0 > 0$. For any $n > C_0$, let $G_{k_l, n} = \min\{n, G_{k_l}\}$. We have

$$\lim_{n \rightarrow +\infty} G_{k_l, n} = G_{k_l}, \quad \lim_{l \rightarrow +\infty} G_{k_l, n} = G^* \quad \text{uniformly for } n > C_0.$$

For a fixed n , $G_{k_l, n}$ is bounded. By the dominated convergence theorem,

$$\lim_{l \rightarrow +\infty} \int_0^1 G_{k_l, n}(\alpha) d\alpha = \int_0^1 G^*(\alpha) d\alpha.$$

Since when $l \rightarrow \infty$, $G_{k_l, n} \rightarrow G^*$ uniformly, we have

$$\begin{aligned} \lim_{l \rightarrow +\infty} \int_0^1 \frac{\nabla U(\varphi_{k_l}) \cdot \Phi}{\sqrt{2E_k - 2U(\varphi_k)}} d\alpha &= \lim_{l \rightarrow +\infty} \lim_{n \rightarrow +\infty} \int_0^1 G_{k_l, n} d\alpha \\ &= \lim_{n \rightarrow +\infty} \lim_{l \rightarrow +\infty} \int_0^1 G_{k_l, n} d\alpha \\ &= \int_0^1 G^*(\alpha) d\alpha = \int_0^1 \frac{\nabla U(\varphi^*) \cdot \Phi}{\sqrt{2E^* - 2U(\varphi^*)}} d\alpha. \end{aligned} \quad (3.32)$$

Because $|\varphi'_k|$ is constant and $|\varphi'_{k_l}| \rightarrow |\varphi^{*'}|$, together with (3.30) and (3.31), we see that φ^* satisfies the Euler-Lagrange equation (3.13) with energy parameter $E = E^*$. Thus φ^* is an extremal of $\hat{S}_{E^*}[\varphi]$.

Remark 3.12. The weak convergence argument for φ'_k is not enough to prove the theorem due to the existence of the term $|\varphi'_k|$. Although we have the uniform L^∞ bound for both, which guarantees $\varphi'_k \rightarrow f$ and $|\varphi'_k| \rightarrow g$, we do not have $g = |f|$ in general.

Theorem 3.10 shows that the graph limit of minimizers of $S_T^{\text{OM}}[\psi]$ can be found by solving the Euler-Lagrange equation of $\hat{S}_E[\varphi]$ with the energy $E^* = \max_{\mathbf{x}} U(\mathbf{x})$. The extremal of $\hat{S}_{E^*}[\varphi]$ always exists, but may not be unique.

Theorem 3.9 shows that it takes infinite time for MPP to pass through a critical point. In general, the time that the MPP spends in any interval is characterized by the function

$$\lambda^* = \frac{\sqrt{2E^* - 2U(\varphi^*)}}{|\varphi^{*'}|}. \quad (3.33)$$

Proposition 3.13. Let $[\alpha_1, \alpha_2] \subset [0, 1]$ be an interval such that $\lambda^*(\alpha) > 0$ for any $\alpha \in [\alpha_1, \alpha_2]$. Then the time that the MPP φ^* takes to go from $\mathbf{x}_1 = \varphi^*(\alpha_1)$ to $\mathbf{x}_2 = \varphi^*(\alpha_2)$ is $\Delta T = \int_{\alpha_1}^{\alpha_2} \lambda^{*-1} d\alpha$.

Proof. By Theorem 3.9 and Proposition 3.11, we may assume $\varphi_k \rightarrow \varphi^*$, $\varphi'_k \rightarrow \varphi^{*'}$ without loss of generality. For any T_k , the relation between φ_k and the minimizer ψ_k of $S_{T_k}[\psi]$ is

$$\varphi_k(\alpha) = \psi_k(\ell_k^{-1}(\alpha)), \quad \text{where } \ell_k(t) = L_k^{-1} \int_0^t |\dot{\psi}_k| dt, \quad L_k = \int_0^{T_k} |\dot{\psi}_k| dt. \quad (3.34)$$

We have $\psi_k(t) = \varphi_k(\ell_k(t))$. Eq. (3.4) shows that the time spent by φ_k from $\mathbf{x}_1^k = \varphi_k(\alpha_1)$ to $\mathbf{x}_2^k = \varphi_k(\alpha_2)$ is

$$\Delta T_k = \int_{t_1}^{t_2} \frac{|\dot{\psi}_k| dt}{\sqrt{2E_k - 2U(\psi_k)}} = \int_{\alpha_1}^{\alpha_2} \frac{|\varphi'_k| d\alpha}{\sqrt{2E_k - 2U(\varphi_k)}}, \quad (3.35)$$

where $t_1 = \ell_k^{-1}(\alpha_1)$, $t_2 = \ell_k^{-1}(\alpha_2)$. Let $k \rightarrow \infty$. We obtain

$$\Delta T = \lim_{k \rightarrow \infty} \Delta T_k = \lim_{k \rightarrow \infty} \int_{\alpha_1}^{\alpha_2} \frac{|\varphi'_k| d\alpha}{\sqrt{2E_k - 2U(\varphi_k)}} = \int_{\alpha_1}^{\alpha_2} \frac{d\alpha}{\lambda^*}. \quad (3.36)$$

□

Proposition 3.13 and Theorem 3.9 show that $\lambda^*(\alpha)$ characterizes the time that the MPP spends at any point α . It takes longer time to pass through points with smaller values of λ^* . Since $|\varphi^{*'}|$ is a constant, the local minima of λ^* correspond to the local maxima of $U(\varphi^*)$ along the MPP. These states will be referred to as the λ -critical state. Note that it does not need to take infinite time to pass through such states.

Remark 3.14. Theorem 3.9 can be readily generalized to non-gradient systems. However, the proof of Proposition 3.11 highly relies on the gradient nature of the system.

4 Comparison with the Freidlin-Wentzell functional

In this section, we make comparisons between the double minimization problems of the OM and FW functionals. We first summarize the differences between these two problems and then give an illustrative example.

4.1 Differences between the FW and OM functionals

When $\varepsilon = 0$, the OM functional reduces to the FW functional. The double minimization problem of the FW functional, which is stated as

$$S^{\text{FW}}(\mathbf{x}_s, \mathbf{x}_f) = \inf_{T>0} \inf_{\psi \in \bar{C}_{\mathbf{x}_s}^{\mathbf{x}_f}[0, T]} S_T^{\text{FW}}[\psi],$$

was studied in [22, 26, 39]. The main results are summarized as follows:

- (1) The infimum occurs at some $T = T^*$. The MPP may not pass through any critical point. $T^* = +\infty$ if and only if the MPP passes through a critical point.
- (2) $S^{\text{FW}}(\mathbf{x}_s, \mathbf{x}_f)$, which is called the local quasi-potential starting from \mathbf{x}_s if \mathbf{x}_s is a steady state, is positive and finite in general.
- (3) The corresponding energy parameter $E(T^*) = 0$ regardless of the value of T^* (finite or infinite). The value of $S^{\text{FW}}(\mathbf{x}_s, \mathbf{x}_f)$ can be obtained by minimizing the geometric functional $\hat{S}_0[\varphi]$, i.e.

$$S^{\text{FW}}(\mathbf{x}_s, \mathbf{x}_f) = \inf_{\varphi \in \bar{C}_{\mathbf{x}_s}^{\mathbf{x}_f}} \hat{S}_0[\varphi].$$

We note that for a prescribed value of T , the corresponding energy E may assume non-zero value.

- (4) Under Assumption 2.9, the minimizer of $S_T^{\text{FW}}[\psi]$ has a subsequence that converges to the minimizer of $\hat{S}_0[\varphi]$ as $T \rightarrow T^*$ in the sense that $\rho(\psi_T, \varphi_0) \rightarrow 0$, where φ_0 is the minimizer of $\hat{S}_0[\varphi]$.

Our results in previous sections generalize the above conclusions for the FW functional to the OM functional. In Proposition 3.7, we showed that the double minimization of the OM functional always occurs at $T^* = +\infty$. Even when neither \mathbf{x}_s nor \mathbf{x}_f is critical, the minimizer must pass through a critical point. The corresponding value of the OM functional $S^{\text{OM}}(\mathbf{x}_s, \mathbf{x}_f)$ is always $-\infty$ when $\varepsilon > 0$. This implies that we cannot define an analog of the quasi-potential as in the Freidlin-Wentzell theory via the minimization of the OM functional. In spite of that, we can still study the graph limit of the minimizers of $S_T^{\text{OM}}[\psi]$ in the configuration space with the help of the Maupertuis principle. Theorem 3.9 showed that the corresponding energy parameter $E(T)$ converges to $E^* = \max_{\mathbf{x} \in \mathbb{R}^d} U(\mathbf{x})$. The minimizer of $S_T^{\text{OM}}[\psi]$ has a subsequence that converges to an extremal of $\hat{S}_{E^*}[\varphi]$. However, the extremal may not be a minimizer of $\hat{S}_{E^*}[\varphi]$. Note that when $\varepsilon \rightarrow 0$, $\max_{\mathbf{x} \in \mathbb{R}^d} U(\mathbf{x}) \rightarrow 0$, then formally $E(T) \rightarrow 0$ as $T \rightarrow +\infty$, which is consistent with the Freidlin-Wentzell theory. The convergence from the OM functional to the FW functional was rigorously studied using the Γ -convergence technique in [31].

In summary, the main differences between the double minimization of the FW and OM functionals are: (1) $S^{\text{FW}}(\mathbf{x}_s, \mathbf{x}_f)$ is finite while $S^{\text{OM}}(\mathbf{x}_s, \mathbf{x}_f)$ is $-\infty$; (2) The minimizer of the FW functional has the

energy $E^* = 0$ while the minimizer of the OM functional has a positive energy; (3) The graph limit of the minimizer of the OM functional is an extremal rather than a minimizer of $\hat{S}_{E^*}[\varphi]$. The second point implies that in the numerical methods, one has to identify the MPP together with the unknown energy E^* at the same time. This is pursued in Section 5.

4.2 An illustrative example

In this section, we present a simple but informative example to illustrate the main results derived earlier for the OM and FW functionals. We consider a 2-D diffusion process with drift $\mathbf{b}(\mathbf{x}) = -\nabla V(\mathbf{x})$, where $V(\mathbf{x}) = \frac{1}{2}|\mathbf{x}|^2$ is a quadratic potential. The path potential $U(\mathbf{x}) = 2\varepsilon - \frac{1}{2}|\mathbf{x}|^2$ has only one critical point $\mathbf{x}_c = 0$, which is also the steady state of the dynamics $\dot{\mathbf{x}} = -\nabla V(\mathbf{x})$.

For any pair of states \mathbf{x}_s , \mathbf{x}_f and fixed $T > 0$, the Euler-Lagrange equation of the OM functional is given by

$$\ddot{\psi}_T(t) - \psi_T(t) = 0, \quad t \in (0, T) \quad (4.1)$$

with the boundary conditions $\psi_T(0) = \mathbf{x}_s$ and $\psi_T(T) = \mathbf{x}_f$. The solution of Eq. (4.1) is given by

$$\psi_T(t) = \mathbf{A}e^t + \mathbf{B}e^{-t}, \quad (4.2)$$

where the vectors \mathbf{A} and \mathbf{B} are given by

$$\mathbf{A} = (e^T - e^{-T})^{-1}(\mathbf{x}_f - \mathbf{x}_s e^{-T}), \quad \mathbf{B} = (e^T - e^{-T})^{-1}(\mathbf{x}_s e^T - \mathbf{x}_f). \quad (4.3)$$

They can be viewed as functions of T . Because $\nabla_y^2 L = I$ is positive definite, ψ_T satisfies strict Legendre-Hadamard condition. So ψ_T is the unique minimizer of $S_T^{\text{OM}}[\psi]$. Since ψ_T is independent of ε , it is also the minimizer of the FW functional $S_T^{\text{FW}}[\psi]$.

Along the path ψ_T , the conservation of energy (3.4) gives

$$\frac{1}{2}|\dot{\psi}_T|^2 + U(\psi_T) = 2\varepsilon - 2\mathbf{A} \cdot \mathbf{B},$$

thus the energy $E = E(T) = 2\varepsilon - 2\mathbf{A} \cdot \mathbf{B}$.

The value of $S_T^{\text{OM}}[\psi_T]$ can be also calculated as

$$\begin{aligned} S_T^{\text{OM}}[\psi_T] &= \int_0^T \left(\frac{1}{2}|\dot{\psi}_T|^2 + \psi_T \cdot \dot{\psi}_T + \frac{1}{2}|\psi_T|^2 \right) dt - 2\varepsilon T \\ &= \frac{1}{2}|\mathbf{x}_f|^2 - \frac{1}{2}|\mathbf{x}_s|^2 - 2\varepsilon T + \frac{1}{2}|\mathbf{A}|^2 (e^{2T} - 1) + \frac{1}{2}|\mathbf{B}|^2 (1 - e^{-2T}). \end{aligned} \quad (4.4)$$

It is straightforward to check that

$$\frac{\partial S_T^{\text{OM}}[\psi_T]}{\partial T} = 2\mathbf{A} \cdot \mathbf{B} - 2\varepsilon = -E(T). \quad (4.5)$$

In what follows we consider two special choices of \mathbf{x}_s and \mathbf{x}_f . Let $\mathbf{x}_s = (R_1 \cos \theta_1, R_1 \sin \theta_1)$ and $\mathbf{x}_f = (R_2 \cos \theta_2, R_2 \sin \theta_2)$. We first consider the case where $\theta_1 = \theta_2 = 0$ and $R_2 > R_1 > 0$, i.e. the two states \mathbf{x}_s and \mathbf{x}_f are on the positive x -axis on the x - y plane, and the initial state \mathbf{x}_s is closer to the origin. In the second case, we set $R_1 = R_2 > 0$ and $0 < \theta_1 < \theta_2 < \pi/2$ where the two states \mathbf{x}_s and \mathbf{x}_f are on the same contour line of the energy $V(\mathbf{x})$. In both cases, we examine the minimizers of the OM and FW functionals in detail.

Case 1: $\theta_1 = \theta_2 = 0$ and $R_2 > R_1 > 0$

Let $\mathbf{x}_s = (x_s, 0)$ and $\mathbf{x}_f = (x_f, 0)$, where $0 < x_s < x_f$. In this case, the vectors $\mathbf{A} = (A, 0)$, $\mathbf{B} = (B, 0)$ in (4.2), thus this is essentially a one-dimensional transition on the x -axis. For simplicity we will use ψ_T to denote the x coordinate of the transition path only.

Figure 1 (left panel) shows the graph of $\partial S_T^{\text{OM}}[\psi_T]/\partial T = 2AB - 2\varepsilon$ (or $-E(T)$) versus T . Denote the two zeros of $\partial S_T^{\text{OM}}[\psi_T]/\partial T$ by T_{\min} and T_{\max} , respectively. Then it is easily seen that $S_T^{\text{OM}}[\psi_T]$ attains a local minimum at $T = T_{\min}$ and a local maximum at $T = T_{\max}$. As $T \rightarrow +\infty$, it follows from (4.3) that $\partial S_T^{\text{OM}}[\psi_T]/\partial T \rightarrow -2\varepsilon$. Thus for sufficiently large T , we have

$$\frac{\partial S_T^{\text{OM}}[\psi_T]}{\partial T} < -\varepsilon < 0,$$

and consequently, $\lim_{T \rightarrow \infty} S_T^{\text{OM}}[\psi_T] = -\infty$, which agrees with the results in Proposition 3.7.

Next we examine the transition path ψ_T and its graph in the configuration space in detail. Note that we have $A > 0$ for any $T > 0$ and $\dot{\psi}_T = Ae^t - Be^{-t}$. To see whether there exists $t \in [0, T]$ such that $\dot{\psi}(t) < 0$, we define

$$f(T) = \frac{B}{A} = \frac{x_s e^T - x_f}{x_f - x_s e^{-T}}.$$

Since $f(T)$ is an increasing function for $T > 0$, there exist unique $T_b > T_a > 0$ such that $f(T_a) = 0$ and $f(T_b) = 1$. A straightforward calculation shows that $\partial S_T^{\text{OM}}[\psi_T]/\partial T$ attains the maximum at $T = T_b$ as shown in Figure 1. We consider the following two cases:

1) $T \leq T_b$. In this case, $B \leq A$. Thus $\dot{\psi}_T \geq 0$ for all $t \in [0, T]$, which implies the system moves from the initial state x_s towards the final state x_f along the path $\psi_T(t)$. The graph of the path is simply the line segment connecting x_s and x_f . Using the normalized arc-length as the parameterization, the path can be expressed as

$$\varphi_E(\alpha) = x_s + L\alpha, \tag{4.6}$$

where $0 \leq \alpha \leq 1$ and $L = x_f - x_s$. Note that although different choices of T correspond to different minimizers ψ_T , they have the same graph in the configuration space.

2) $T > T_b$. In this case, we have $B > A$ and there exists a unique $t^* = \ln \sqrt{B/A} \in [0, T]$ such that $\dot{\psi}_T(t^*) = 0$. Furthermore we have $\dot{\psi}_T < 0$ when $t \in [0, t^*)$ and $\dot{\psi}_T > 0$ when $t \in (t^*, T]$. It follows that, along the transition path, the system moves towards the origin until $t = t^*$ then it turns back and moves towards the final state x_f . The turning point is given by $x_c = \psi_T(t^*) = 2\sqrt{AB} < x_s$.

The mapping from ψ_T on $[0, T]$ to φ_E on $[0, 1]$ is done as follows. We define the normalized arc-length parameterization as

$$\alpha = \ell(t) = \begin{cases} L^{-1}(x_s - \psi_T(t)), & 0 \leq t \leq t^* \\ L^{-1}(x_s - 2x_c + \psi_T(t)), & t^* \leq t \leq T, \end{cases} \tag{4.7}$$

where L is the arc-length of the path

$$L = \int_0^T |\dot{\psi}_T| dt = - \int_0^{t^*} \dot{\psi}_T dt + \int_{t^*}^T \dot{\psi}_T dt = x_f + x_s - 2x_c.$$

Then $\psi_T(t)$ is mapped to

$$\varphi_E(\alpha) = \begin{cases} x_s - L\alpha, & 0 \leq \alpha \leq \alpha^* \\ 2x_c - x_s + L\alpha, & \alpha^* \leq \alpha \leq 1, \end{cases} \tag{4.8}$$

where $\alpha^* = \ell(t^*) = L^{-1}(x_s - x_c)$.

The graph φ_E in (4.8) depends on T . In particular, the turning point x_c is a function of T ,

$$x_c = 2\sqrt{AB} = (2x_s x_f \cosh T - x_s^2 - x_f^2)^{1/2} / \sinh T.$$

It is easily seen that as $T \rightarrow +\infty$, $x_c \rightarrow 0$, i.e. the turning point converges to the critical point. This shows that the graph limit of the MPP will pass through a critical point even when x_s and x_f are not at the steady state of $\dot{x} = -\nabla V(x)$. Furthermore, the energy $E(T) \rightarrow E^* = 2\varepsilon$ as $T \rightarrow +\infty$. In this limit, φ_E converges to

$$\varphi_{E^*}(\alpha) = \begin{cases} x_s - L\alpha, & 0 \leq \alpha \leq (x_f + x_s)^{-1} x_s, \\ L\alpha - x_s, & (x_f + x_s)^{-1} x_s \leq \alpha \leq 1. \end{cases} \tag{4.9}$$

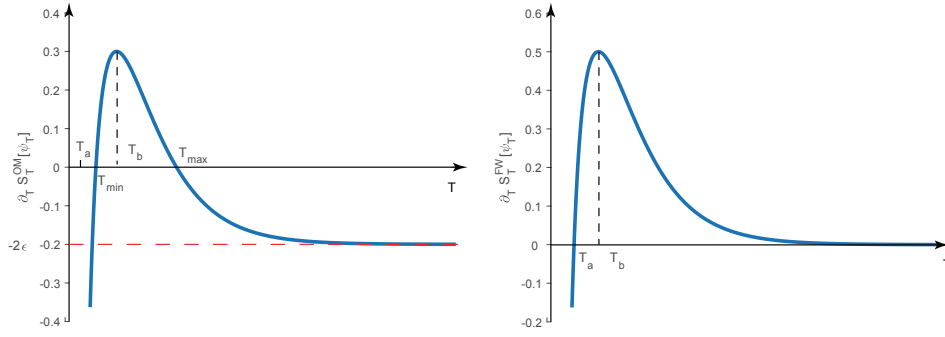


Figure 1 The plot of $\partial S_T[\psi_T]/\partial T$ (or $-E(T)$) versus T for the Onsager-Machlup functional (left panel) and the Freidlin-Wentzell (right panel), where $x_s = 1, x_f = 2, \varepsilon = 0.1$. $T_a < T_b$ satisfy $f(T_a) = 0, f(T_b) = 1$. T_{\min} and T_{\max} are two zeros of $\partial S_T^{\text{OM}}[\psi_T]/\partial T$.

The geometric functional corresponding to $E^* = 2\varepsilon$ is given by

$$\hat{S}_{E^*}[\varphi] = \int_0^1 |\varphi| |\varphi'| \, d\alpha.$$

The corresponding strong form of the Euler-Lagrange equation is

$$|\varphi|^2 \varphi'' + (\varphi \cdot \varphi') \varphi' - |\varphi'|^2 \varphi = 0. \quad (4.10)$$

It is easy to see that the graph limit φ_{E^*} with the turning point $\mathbf{x}_c = 0$ is a weak solution of (4.10), thus an extremal of the functional $\hat{S}_{E^*}[\varphi]$. This verifies the result obtained in Theorem 3.10. To further check whether φ_{E^*} is the global minimizer of $\hat{S}_{E^*}[\varphi]$, we compare it with the following function

$$\tilde{\varphi}(\alpha) = x_s + \tilde{L}\alpha, \quad \alpha \in [0, 1],$$

where $\tilde{L} = x_f - x_s$. This is the graph of the path obtained when $T \leq T_b$. A direct calculation yields

$$\hat{S}_{E^*}[\tilde{\varphi}] = \frac{1}{2}(x_f^2 - x_s^2).$$

In comparison,

$$\hat{S}_{E^*}[\varphi_{E^*}] = \frac{1}{2}(x_f^2 + x_s^2) > \hat{S}_{E^*}[\tilde{\varphi}].$$

Thus φ_{E^*} is only an extremal of $\hat{S}_{E^*}[\varphi]$, but not its global minimizer.

Next we compare the results obtained above for the OM functional with the FW functional. For the FW functional, since $\varepsilon = 0$, we have $\partial S_T^{\text{FW}}[\psi_T]/\partial T = 2AB$. The right panel of Figure 1 shows the graph of $\partial S_T^{\text{FW}}[\psi_T]/\partial T$ versus T . The only zero of $\partial S_T^{\text{FW}}[\psi_T]/\partial T = 0$ occurs at $T = T_a$, at which $S_T^{\text{FW}}[\psi_T]$ attains the global minimum. The graph of the corresponding transition path is the one in (4.6), which has the action

$$S_{T_a}^{\text{FW}}[\psi_{T_a}] = x_f^2 - x_s^2 = 2V(\mathbf{x}_f) - 2V(\mathbf{x}_s).$$

In comparison, when $T \rightarrow \infty$, the graph of the transition path converges to the one given in (4.9) with the action

$$\lim_{T \rightarrow +\infty} S_T^{\text{FW}}[\psi_T] = x_f^2 = 2V(\mathbf{x}_f) - 2V(\mathbf{0}),$$

which is obviously larger than $S_{T_a}^{\text{FW}}[\psi_{T_a}]$.

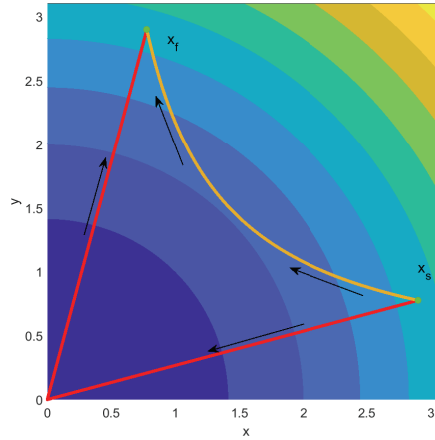


Figure 2 (Color Online). The minimizer of the FW and OM functionals from \mathbf{x}_s to \mathbf{x}_f , where $R = 3$, $\theta_1 = \pi/12$, $\theta_2 = 5\pi/12$, $\varepsilon = 0.1$. Yellow curve: the minimizer of the FW functional. Red line: the minimizer of the OM functional. The background colors show the contour of $V(\mathbf{x})$.

Case 2: $R_1 = R_2 = R > 0$ and $0 < \theta_1 < \theta_2 < \pi/2$

In this case, we illustrate the different transition behaviors modeled by the OM and FW functionals between the two states $\mathbf{x}_s = (R \cos \theta_1, R \sin \theta_1)$, $\mathbf{x}_f = (R \cos \theta_2, R \sin \theta_2)$. The two states lie on the same contour line of $V(\mathbf{x})$ with $V(\mathbf{x}_s) = V(\mathbf{x}_f) = R^2/2$.

Let us consider the OM functional first. As in case 1, the fact that

$$\frac{\partial S_T^{\text{OM}}[\psi_T]}{\partial T} = -E \rightarrow -2\varepsilon < 0$$

as $T \rightarrow +\infty$ implies that the infimum of $S_T^{\text{OM}}[\psi_T]$ occurs when $T \rightarrow +\infty$. To examine if the transition path passes through the origin, we consider the distance of the minimizer ψ_T to the origin. For any given T , we have

$$\frac{d}{dt} |\psi_T|^2 = 2|\mathbf{A}|^2 e^{2t} - 2|\mathbf{B}|^2 e^{-2t}.$$

The solution of $d|\psi_T|^2/dt = 0$ is $t^* = \ln(|\mathbf{B}|/|\mathbf{A}|)/2 > 0$. In addition, we have $d^2|\psi_T|^2/dt^2 > 0$ for all t , therefore, $|\psi_T|$ attains its minimum at $t = t^*$, i.e. $\psi_T(t^*)$ is the state along the path which is the closest to the origin. This shortest distance is given by

$$|\psi_T|_{\min}^2 = |\psi_T|^2(t^*) = 2|\mathbf{A}||\mathbf{B}| + 2\mathbf{A} \cdot \mathbf{B}, \tag{4.11}$$

which converges to 0 as $T \rightarrow \infty$. Therefore, the graph limit of the transition path passes through the critical point $\mathbf{x} = 0$. A typical path is shown in Figure 2.

For the FW functional, the minimum of $S_T^{\text{FW}}[\psi_T]$ is attained at $T = T_c$, the solution to $\partial S_T^{\text{FW}}[\psi_T]/\partial T = 0$, or explicitly,

$$T_c = \cosh^{-1} \left(\frac{1}{\cos(\theta_2 - \theta_1)} \right).$$

The corresponding action is given by $S_{T_c}^{\text{FW}}[\psi_{T_c}] = 4R^2 \sin(\theta_2 - \theta_1)$. The shortest distance from the path ψ_{T_c} to the origin can be computed using (4.11), which yields

$$|\psi_{T_c}|_{\min}^2 = R^2 \cos(\theta_2 - \theta_1) \leq R^2.$$

This shows that the minimizer of the FW functional, ψ_{T_c} , has a positive distance from the origin, and the distance is smaller than R . A typical graph of the transition path is shown in Figure 2. Note that it is not along the contour of $V(\mathbf{x})$.

5 Numerical method

Based on the insights gained from the theoretical analysis in previous sections, we design an energy-climbing geometric minimization method to compute the graph limit of the minimizer of the OM functional when T goes to infinity.

The graph limit of the minimizer satisfies the Euler-Lagrange equation (3.14), with the kinetic energy $K_E = E - U(\varphi)$ and $E = \max_{\alpha} U(\varphi(\alpha))$. This is a highly nonlinear equation. We propose to use the following steepest decent like dynamics to find the solution:

$$\begin{aligned} \frac{\partial \varphi}{\partial s} &= 2K(s, \alpha)\varphi'' + |\varphi'|^2 (I - \hat{\tau} \otimes \hat{\tau}) \cdot \nabla U(\varphi) + \lambda \hat{\tau}, \quad \alpha \in (0, 1), \quad s > 0 \\ \varphi(s, 0) &= \mathbf{x}_s, \quad \varphi(s, 1) = \mathbf{x}_f, \quad \text{and} \quad (|\varphi'|)' = 0 \end{aligned} \quad (5.1)$$

with initial condition $\varphi(0, \alpha) = \varphi^0(\alpha)$, where λ is a Lagrange multiplier to ensure the constraint $(|\varphi'|)' = 0$, and

$$K(s, \alpha) := E(s) - U(\varphi(s, \alpha)) \quad \text{and} \quad E(s) := \max_{\alpha} U(\varphi(s, \alpha)). \quad (5.2)$$

Here s denotes the artificial relaxation time.

The well-posedness and long time behavior of Eq. (5.1) is not well-understood yet due to the nonlinearity and degeneracy of $K(s, \alpha)$ at $\alpha_c = \operatorname{argmax}_{\alpha} U(\varphi)$. We will leave this problem to our future studies. Nevertheless, provided the dynamical system (5.1) reaches a steady state as $s \rightarrow \infty$, the steady-state solution solves (3.14), thus gives the graph limit of the minimizer of the OM functional.

We use (5.1) to construct numerical schemes. We first semi-discretize Eq. (5.1) with respect to the relaxation time s . Using an explicit time-stepping with stepsize δs , we get

$$\varphi^{n+1} = \varphi^n + \delta s \left(2K_n(\alpha)(\varphi^n)'' + |(\varphi^n)'|^2 (I - \hat{\tau}^n \otimes \hat{\tau}^n) \cdot \nabla U(\varphi^n) \right) + \lambda^{n+1} \hat{\tau}^{n+1}, \quad (5.3)$$

where $\varphi^n(\alpha)$ is the numerical approximation of $\varphi(n\delta s, \alpha)$ and

$$K_n(\alpha) := E_n - U(\varphi^n), \quad E_n := \max_{\alpha} U(\varphi^n(\alpha)). \quad (5.4)$$

The scheme (5.3) is equivalent to first obtain $\tilde{\varphi}^{n+1}$ by

$$\tilde{\varphi}^{n+1} = \varphi^n + \delta s \left(2K_n(\alpha)(\varphi^n)'' + |(\varphi^n)'|^2 (I - \hat{\tau}^n \otimes \hat{\tau}^n) \cdot \nabla U(\varphi^n) \right), \quad (5.5)$$

then get φ^{n+1} by reparameterizing $\tilde{\varphi}^{n+1}$ with equi-arclength condition.

For a given φ^0 , the scheme (5.3) generates a sequence of paths $\{\varphi^n\}$ and the corresponding energy $\{E_n\}$. We have the following theorem concerning the properties of the above numerical scheme.

Proposition 5.1. *Suppose $\varphi^0(\alpha) \in C^\infty[0, 1]$, $U(\mathbf{x}) \in C^\infty(\mathbb{R}^d)$, then $\varphi^n(\alpha) \in C^\infty[0, 1]$. When δs is sufficiently small, the sequence $\{E_n\}$ generated using (5.3) is nondecreasing. Moreover, if φ^n converges to a steady state φ^* , then $E_n \rightarrow E_c$, and φ^* solves the Euler-Lagrange equation (3.14) with $E = E_c$. Here, $E_c = U(\varphi^*(\alpha^*))$ for some $\alpha^* \in [0, 1]$. $\mathbf{x}^* = \varphi^*(\alpha^*)$ satisfies the condition $\nabla U(\mathbf{x}^*) = 0$.*

Proof. Because φ^0 and U are smooth, we have $\varphi^1 \in C^\infty$ from (5.3). The fact that $\varphi^n \in C^\infty$ can be deduced by induction.

Let $\alpha_n = \inf\{\alpha \in [0, 1] | U(\varphi^n(\alpha)) = \max_{\alpha} U(\varphi^n(\alpha))\}$. We have $E_n = U(\varphi^n(\alpha_n))$. We first assume $\alpha_n \in (0, 1)$. If $\nabla U(\varphi^n(\alpha_n)) = 0$, then there exists $\beta_n \in (0, 1)$ such that $\varphi^{n+1}(\beta_n) = \tilde{\varphi}^{n+1}(\alpha_n) = \varphi^n(\alpha_n)$ by (5.3) and (5.5).

So $E_{n+1} \geq U(\varphi^{n+1}(\beta_n)) = E_n$. If $\nabla U(\varphi^n(\alpha_n)) \neq 0$, we have

$$\begin{aligned} E_{n+1} - E_n &\geq U(\tilde{\varphi}^{n+1}(\alpha_n)) - U(\varphi^n(\alpha_n)) \\ &= \nabla U(\varphi^n(\alpha_n)) \cdot (\tilde{\varphi}^{n+1}(\alpha_n) - \varphi^n(\alpha_n)) + O(|\tilde{\varphi}^{n+1}(\alpha_n) - \varphi^n(\alpha_n)|^2). \end{aligned} \quad (5.6)$$

When $\alpha = \alpha_n$, $\nabla U \cdot (\varphi^n)' = 0$. According to scheme (5.5), $\tilde{\varphi}^{n+1}(\alpha_n) - \varphi^n(\alpha_n) = \delta s |(\varphi^n)'|^2 \nabla U(\varphi^n(\alpha_n))$, $|\tilde{\varphi}^{n+1}(\alpha_n) - \varphi^n(\alpha_n)| = O(\delta s)$. From (5.6), we have

$$E_{n+1} - E_n \geq |(\varphi^n)'|^2 |\nabla U(\varphi^n(\alpha_n))|^2 \delta s + O(\delta s^2) \geq 0 \quad (5.7)$$

when δs^2 is sufficiently small. So $\{E_k\}$ is nondecreasing.

If $\alpha_n = 0$, $E_{n+1} = \max U(\varphi^{n+1}(\alpha)) \geq U(\varphi^{n+1}(0)) = U(\mathbf{x}_s) = U(\varphi^n(0)) = E_n$. So $E_{n+1} \geq E_n$ still holds. The case $\alpha_n = 1$ is similar. In all, we have shown that $\{E_k\}$ is nondecreasing.

If the scheme reaches a steady state φ^* , then E_n converges to some E_c by the definition $E_n = \max_{\alpha} U(\varphi^n(\alpha))$ and the assumption that φ^n converges. The limit φ^* solves

$$2K_{E_c}(\varphi^*)(\varphi^*)'' + |(\varphi^*)'|^2 (I - \hat{\tau} \otimes \hat{\tau}) \cdot \nabla U(\varphi^*) + \lambda \hat{\tau} = 0, \quad (5.8)$$

subject to the constraint $(|(\varphi^*)'|)' = 0$, where

$$K_{E_c}(\varphi^*) := E_c - U(\varphi^*), \quad E_c := \max_{\alpha} U(\varphi^*(\alpha)).$$

Take inner product of both sides of (5.8) with $\hat{\tau}$, we get the Lagrange multiplier $\lambda(\alpha) \equiv 0$ and thus φ^* solves Eq. (3.14) with $E = E_c$. Let $\alpha^* = \arg \max_{\alpha} U(\varphi^*(\alpha))$. From (5.8), we have $\nabla U(\varphi^*(\alpha^*)) = (\hat{\tau} \cdot \nabla U(\varphi^*(\alpha^*)))\hat{\tau} = 0$. \square

Remark 5.2. A careful inspection of the proof shows that the properties on E_n and φ^* hold also for non-gradient systems as long as the path has second order differentiability.

Let us re-examine the iteration at $\alpha = \alpha_n$. Since $E_n = U(\varphi^n(\alpha_n))$, we have $\nabla U \cdot (\varphi^n)' = 0$, and the iteration in (5.5) reduces to $\tilde{\varphi}^{n+1}(\alpha_n) = \varphi^n(\alpha_n) + \delta s |(\varphi^n)'|^2 \nabla U(\varphi^n(\alpha_n))$. This can be viewed as a steepest ascent method to find the maximum of $U(\mathbf{x})$ with step size $\delta s |(\varphi^n)'|^2$. The convergence result shows that $\varphi^n(\alpha_n)$ converges to a point with $\nabla U = 0$. So the iteration (5.3) can be considered as a combination of a relaxation method to solve the Euler-Lagrange equation and the steepest ascent method to find the maximum of $U(x)$.

In practical computations, the path φ^n is discretized into a collection of discrete states, $\varphi_j^n = \varphi^n(jh)$, where $h = 1/N$ and $j = 0, 1, \dots, N$, and the spatial derivatives of φ^n are discretized using the central difference formula. This gives the following algorithm:

It is worth noting that the explicit numerical scheme in the above algorithm can be replaced by a semi-implicit scheme, in which the spatial derivative φ'' is evaluated at $(n+1)\delta s$:

$$\varphi_j'' \approx D^2 \tilde{\varphi}_j^{n+1} = (\tilde{\varphi}_{j+1}^{n+1} - 2\tilde{\varphi}_j^{n+1} + \tilde{\varphi}_{j-1}^{n+1})/h^2.$$

This will be a more stable scheme in practice. At each step, this semi-implicit scheme requires solving a tri-diagonal linear system, but allows a relatively large time stepsize. Such linear systems can be solved by fast algorithms, e.g. the Thomas algorithm, whose computational cost is comparable to the cost of the explicit scheme.

The purpose of step (4) in EGMA is to redistribute the discrete images so that they are equally spaced along the path. This can be done using interpolation techniques as introduced in the string method [10, 12]. One simple strategy that uses the linear interpolation is illustrated as follows.

The stopping criterion in EGMA is based on the rate of change of φ^n . In the computations below, we set the tolerance $TOL = 10^{-6}$.

Remark 5.3. EGMA can also be applied to non-gradient type of systems by solving the following semi-discrete scheme

$$\varphi^{n+1} = \varphi^n + \delta s \left(2K_n(\varphi^n)(\varphi^n)'' + \sqrt{2K_n(\varphi^n)}(\nabla \mathbf{b}^T - \nabla \mathbf{b}) \cdot (\varphi^n)' \right)$$

Algorithm 1 Energy climbing geometric minimization algorithm (EGMA)

- (1) Given $\varphi_j^0 = \varphi^0(jh)$ for $j = 0, 1, \dots, N$ and $h = 1/N$. Set $n = 0$.
- (2) For path φ_j^n , let $E_n = \max_j U(\varphi_j^n)$ and compute

$$\begin{aligned} D\varphi_j^n &= (\varphi_{j+1}^n - \varphi_{j-1}^n)/(2h), \\ D^2\varphi_j^n &= (\varphi_{j+1}^n - 2\varphi_j^n + \varphi_{j-1}^n)/h^2, \end{aligned}$$

for $j = 1, 2, \dots, N - 1$.

- (3) Let $\tilde{\varphi}_0^{n+1} = \mathbf{x}_s$, $\tilde{\varphi}_N^{n+1} = \mathbf{x}_f$. Then compute

$$\tilde{\varphi}_j^{n+1} = \varphi_j^n + \delta s \left[(2E_n - 2U)D^2\varphi_j^n + |D\varphi_j^n|^2 \nabla U - (\nabla U \cdot D\varphi_j^n)D\varphi_j^n \right]$$

for $j = 1, 2, \dots, N - 1$. Here U and ∇U are both evaluated at φ_j^n .

- (4) Compute φ_j^{n+1} by interpolating $\{\tilde{\varphi}_j^{n+1}\}$ based on the equi-arclength constraint.
- (5) Terminate the iteration if $|\varphi^{n+1} - \varphi^n|/\delta s < TOL$, where TOL is a prescribed tolerance.
- (6) Set $n := n + 1$ and goto step 2.
-

Algorithm 2 Equal-arclength reparametrization

- (1) Let $L(0) = 0$ and

$$L(j) = \sum_{m=1}^j |\tilde{\varphi}_m^{n+1} - \tilde{\varphi}_{m-1}^{n+1}|, \quad j = 1, 2, \dots, N.$$

- (2) Compute the equally spaced arc-length parameter $l(j) = jL(N)/N$ for $j = 0, 1, \dots, N$.
- (3) For each $j = 1, 2, \dots, N - 1$, find $i \in \{0, 1, \dots, N - 1\}$ such that $L(i) < l(j) \leq L(i + 1)$, then compute φ_j^{n+1} as follows:

$$\varphi_j^{n+1} = \tilde{\varphi}_i^{n+1} + (l(j) - L(i)) \frac{\tilde{\varphi}_{i+1}^{n+1} - \tilde{\varphi}_i^{n+1}}{|\tilde{\varphi}_{i+1}^{n+1} - \tilde{\varphi}_i^{n+1}|}.$$

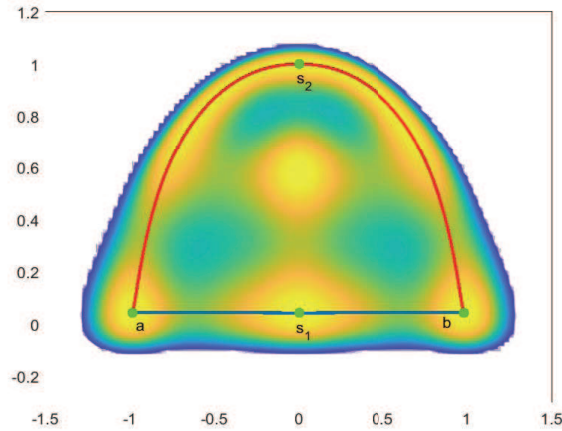


Figure 3 (Color Online). The heat plot of $V(x, y)$ and two transition paths when $\varepsilon = 0$ (the FW theory). The blue and red lines correspond to the direct and circular transition paths, respectively. The green dots correspond to the minima (a and b) and saddle points (s_1 and s_2) of $V(x, y)$. The two saddle points s_1 and s_2 have the same energy when $\gamma \approx 12.16$. The background color indicates the value of V , where the yellow color corresponds to small values of V , and blue color corresponds to large values of V .

$$+ |(\varphi^n)'|^2 (I - \hat{\tau}^n \otimes \hat{\tau}^n) \cdot \nabla U(\varphi^n) + \lambda^{n+1} \hat{\tau}^{n+1}, \quad (5.9)$$

where K_n is defined in (5.4). We remark that in this semi-discrete scheme, the smoothness of φ^n does not guarantee the smoothness of φ^{n+1} . However, this does not introduce any difficulty in applying the full discretization scheme of (5.9) in numerical computations.

6 Numerical examples

We apply the numerical method to three examples: an example in 2D, the re-arrangement of seven-atom cluster, and the Maier-Stein model.

In these examples, we use

$$\lambda(\alpha) = \frac{\sqrt{2E - 2U(\varphi(\alpha))}}{|\varphi'|}$$

as the indicator of λ -critical states. Here, $\varphi(\alpha)$ is the path we get after iteration, $E = \max_{\alpha} U(\varphi)$. The local minima of $\lambda(\alpha)$ are λ -critical states. When $\varepsilon = 0$, metastable states and transition states are all λ -critical states ($\lambda(\alpha) = 0$ at these states). As proved in proposition 3.13, the transition spent longer time at these states than others.

6.1 A 2D example

We consider the potential V in two-dimensional space:

$$\begin{aligned} V(x, y) = & 4(x^2 + y^2 - 1)^2 y^2 - \exp(-4((x-1)^2 + y^2)) - \exp(-4((x+1)^2 + y^2)) \\ & + \exp(8(x-1.5)) + \exp(-8(x-1.5)) + \exp(\gamma(y+0.25)) + 0.2 \exp(-8x^2). \end{aligned}$$

The potential $V(x, y)$ has two minima at a and b , and two saddle points at s_1 and s_2 , as shown in Figure 3. For a properly chosen γ ($\gamma \approx 12.16$), the two saddle points have the same potential energy. The FW functional (i.e. when $\varepsilon = 0$) has two minima for the transition between a and b , one being a straight line through s_1 and the other a circular path through s_2 . The two paths have the same action, and they are also the minimum energy paths for the potential V .

Notice that when $\varepsilon = 0$, all critical points of V , i.e. the states \mathbf{x} with $\nabla V(\mathbf{x}) = 0$, are critical points (maxima) of U . When $\varepsilon > 0$ but small, the local/global maxima of U are still in the neighborhood of

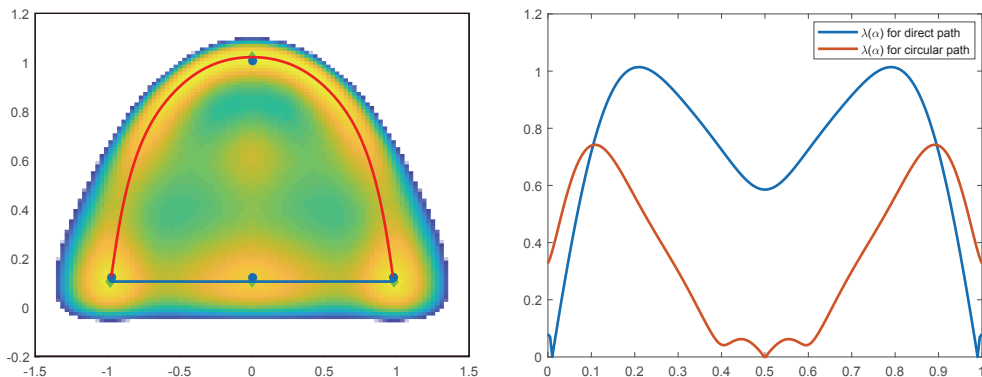


Figure 4 (Color Online). Left panel: Two solutions of the Euler-Lagrange equation (3.14) with $\varepsilon = 0.05$. The blue straight line passes through local maxima of $U(x, y)$ close to the minima of V . The red circular line passes through the global maxima of U that are close to the upper saddle of V . The background is the heat plot of U , in which the yellow color corresponds to large values of U , and blue color corresponds to small values of U , which is opposite to Figure 3. The blue circles indicate the minima and saddle points of V , and the green diamonds are local maxima of U . Right panel: The indicator $\lambda(\alpha)$ of two paths. The blue and red curves correspond to the straight and circular paths, respectively. The indicator $\lambda = 0$ corresponds to the states with $U(\varphi) = E_c$.

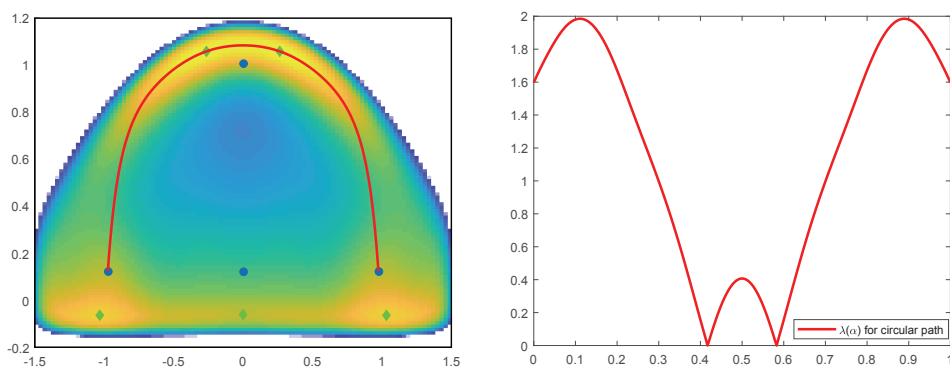


Figure 5 (Color Online). Left panel: The circular transition path when $\varepsilon = 0.5$. The path passes through two critical points that are away from the upper saddle point of V . The background is the heat plot of U . Right panel: The indicator $\lambda(\alpha)$. The zeros of λ corresponds to two critical points.

the critical points of V . For example, as shown in Figure 4, U attains the maxima near the minima, the saddle points and the maxima of V when $\varepsilon = 0.05$. Among these maxima of U , the one near s_2 is the global maximum, thus the critical point of U .

For $\varepsilon = 0.05$, we solved (5.1) for the transition path between a and b using EGMA. Using different initial path in the iteration, we obtained two paths connecting a and b : one passing through the three local maxima of U near a , s_1 and b , respectively, and the other passing through the global maxima of U near s_2 . Both satisfies the Euler-Lagrange equation (3.14), thus are extremals of $\hat{S}_E[\varphi]$. However, the two paths have different energy: $E_c \approx 1.0849$ for the first one and $E_c \approx 1.5516$ for the second one. These energy values are also the maximum of U along the corresponding path. From the analysis in previous sections, the path passing through the global maximum of U is the graph limit of the minimizers of $S_T^{OM}[\psi]$ as $T \rightarrow \infty$.

When ε is relatively large, on the other hand, U may have a different landscape. For example, when $\varepsilon = 0.5$, the critical point of U near s_2 disappears and two new critical points appear slightly far away from this saddle point. Figure 5 shows that the converged path passes through these two critical points with energy $E_c \approx 23.9939$. This result shows that with a finite ε , the OM functional may give quite different λ -critical states compared with the transition states for the zero noise limit.

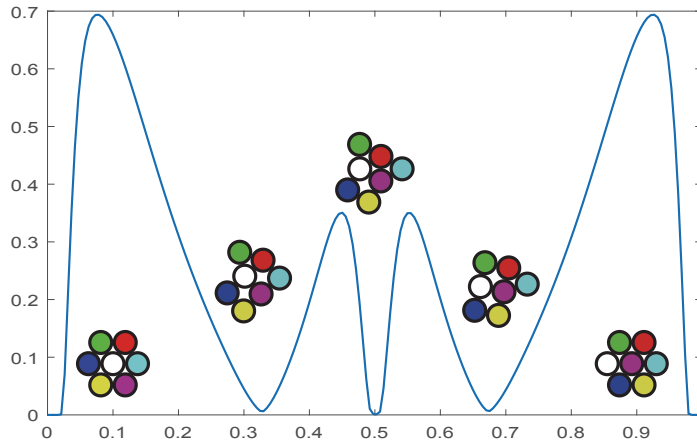


Figure 6 (Color Online). The indicator $\lambda(\alpha)$ for the MPP and the corresponding λ -critical states when $\varepsilon = 0$ (i.e. the FW functional). The λ -critical states are the states where λ attains local minima.

6.2 Rearrangement of a seven-atom cluster

In this example, we consider the rearrangement of a cluster consisting of seven atoms. This problem was studied in [7, 10, 30] using different approaches. The positions of the atoms are denoted by $\mathbf{x}^{(i)} \in \mathbb{R}^2, i = 1, 2, \dots, 7$. The state of the system in the configuration space is represented by a vector $\mathbf{x} = (\mathbf{x}^{(1)}, \dots, \mathbf{x}^{(7)}) \in \mathbb{R}^{14}$. The interactions between the atoms are modeled by the Lennard-Jones potential:

$$V(\mathbf{x}) = 2\delta \sum_{i \neq j} \left(\frac{\sigma}{r_{ij}} \right)^{12} - \left(\frac{\sigma}{r_{ij}} \right)^6, \quad (6.1)$$

where $\delta, \sigma > 0$, $r_{ij} = |\mathbf{x}^{(i)} - \mathbf{x}^{(j)}|$ is the distance between $\mathbf{x}^{(i)}$ and $\mathbf{x}^{(j)}$. The global minimum of this potential corresponds to the configuration in which an atom is surrounded by the other six in a hexagonal shape. We compute the pathway along which the central atom (colored in white in Figs Figure 6-Figure 9) migrates to the surface using EGMA with different values of ε . We use $N = 192$ points to discretize the path, and take $\delta = \sigma = 1$ in the potential.

We first show the transition path and transition states inferred by the FW theory, i.e. the case when $\varepsilon = 0$, in Figure 6. The curve in Figure 6 shows the indicator λ . As shown in the FW theory [22], the metastable states and transition states along the transition path are given by the points with $\lambda(\alpha) = 0$. They are all λ -critical states. We plot the configuration of each λ -critical state in Figure 6. These λ -critical states are also the minima or saddle points of V and they are the same as those obtained in the earlier work [7, 10].

Figure 7 shows the indicator $\lambda(\alpha)$ along the path obtained with $\varepsilon = 0.01$. As we have mentioned, each local minimum of λ corresponds to a λ -critical state. These states have different interpretations. The initial and final states, which correspond to the case where one atom is surrounded by the other six, are the minimum of λ . This means that they are more stable than the other three λ -critical states. Similarly, the symmetric state (observe with a small tilt angle) in the middle of the path is more stable than another two asymmetric ones aside. Because ε is quite small here, the λ -critical state we get are similar as those obtained by FW theory.

We also applied EGMA to the cases $\varepsilon = 0.1$ and $\varepsilon = 1$, and the numerical results are shown in Figs. Figure 8 and Figure 9, respectively. In Figure 8, we observe similar transition pattern as in the case $\varepsilon = 0.01$. Although the critical points of U that the path goes through are slightly perturbed from the initial and final states, their configurations are qualitatively indistinguishable from those states. The symmetric state in the middle remains to be a λ -critical state as a local minimum of the indicator λ . In the case $\varepsilon = 1$ (shown in Fig, Figure 9), the two asymmetric states inside replace the initial and final states as the critical states. Furthermore, the middle symmetric state is no longer a λ -critical state.

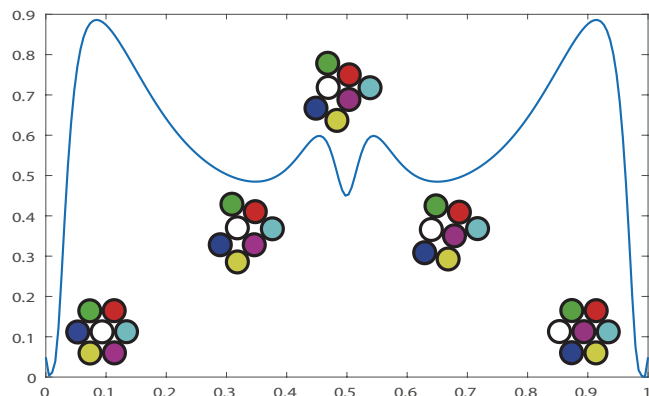


Figure 7 (Color Online). The indicator $\lambda(\alpha)$ for the MPP and the corresponding λ -critical states when $\varepsilon = 0.01$. The transition behavior resembles the case when $\varepsilon = 0$.

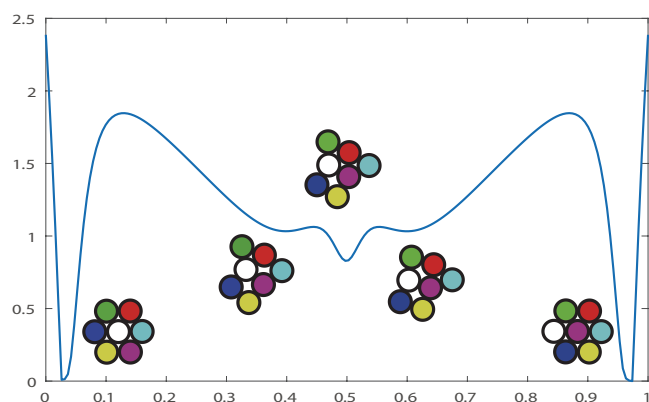


Figure 8 (Color Online). The indicator $\lambda(\alpha)$ for the MPP and the corresponding λ -critical states when $\varepsilon = 0.1$. The qualitative behavior remains unchanged compared with the case $\varepsilon = 0.01$.

During the transition, the atoms have slight overlapping due to strong noise perturbations. Similar phenomena was also observed in [30].

6.3 The Maier-Stein model

In this example, we apply the numerical method to a non-gradient system. The Maier-Stein model is a standard non-gradient diffusion process that has been carefully studied [27]. The drift term \mathbf{b} in Eq. (1.1) is

$$\mathbf{b}(x, y) = \begin{bmatrix} x - x^3 - \beta xy^2 \\ -(1 + x^2)y \end{bmatrix}, \quad (6.2)$$

where $\beta > 0$ is a parameter. The system is of the gradient type only when $\beta = 1$. For any $\beta > 0$, the deterministic dynamics $\dot{\mathbf{x}} = \mathbf{b}(\mathbf{x})$ has two stable fixed points at $(\pm 1, 0)$ and one saddle point at $(0, 0)$. The path potential $U(x, y)$ is given by

$$U(x, y) = 4\varepsilon x^2 + \varepsilon \beta y^2 - \frac{1}{2}[(x - x^3 - \beta xy^2)^2 + (1 + x^2)^2 y^2]. \quad (6.3)$$

In the limit $\varepsilon \rightarrow 0$, Maier and Stein studied the transition path from $(-1, 0)$ to $(1, 0)$ for various β , and found two transition patterns [27]. When $\beta < 4$, the path is the line segment connecting $(-1, 0)$ and $(1, 0)$, while when $\beta > 4$, the path is composed of two parts: one from $(-1, 0)$ to $(0, 0)$ following the curved heteroclinic orbit and the other from $(0, 0)$ to $(0, 1)$ following the line segment.

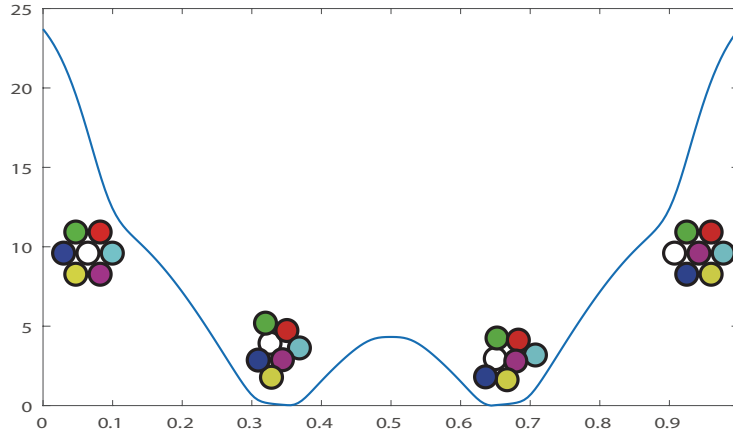


Figure 9 (Color Online). The indicator $\lambda(\alpha)$ for the MPP and the corresponding λ -critical states when $\varepsilon = 1$. The two asymmetric states shown in the figure replace the initial and final states as the critical states. The atoms slightly overlap due to the strong noise.

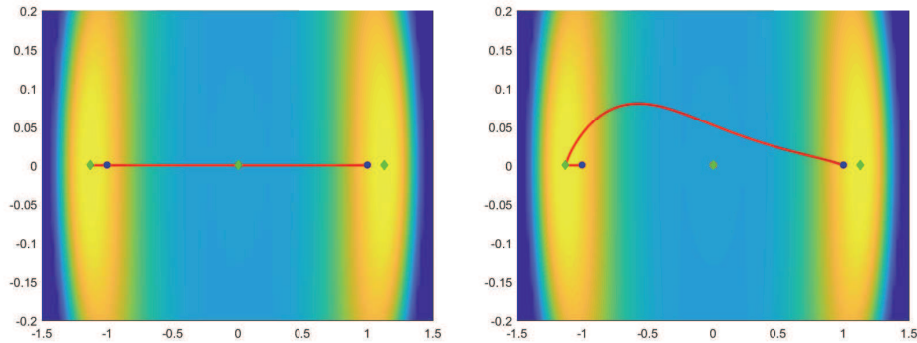


Figure 10 (Color Online). The MPP of the OM functional for the Maier-Stein model, where $x_s = (-1, 0)$, $x_f = (1, 0)$ and $\varepsilon = 0.1$. Left panel: $\beta = 3.4$. Right panel: $\beta = 3.5$. Blue circles are fixed points of $\dot{x} = \mathbf{b}(x)$. Green diamonds are local maximum points of $U(x)$. The background is the heat map of $U(x)$.

Using EGMA, we can study the same transition for $\varepsilon > 0$. Figure 10 shows the numerical results for $\varepsilon = 0.1$. We also obtain two types of transition paths. However, the critical value of β that separates the two patterns is lowered to a value between 3.4 and 3.5. More interestingly, as predicted by the theoretical result, the paths now pass through a critical point $(x_c, 0)$ which is located to the left of $(-1, 0)$.

The critical point $(x_c, 0)$ can be calculated explicitly as $x_c^2 = (2 + \sqrt{1 + 24\varepsilon})/3$. The corresponding energy is given by $E_c = U(x_c, 0)$. This helps us study the convergence property of our EGMA. We set $\varepsilon = 0.1$, $\delta s = 0.01$, $\beta = 10$ and run 500 iterations with different spatial resolution N . We compute the difference between E_c and E_n in each iteration step. The convergence history of the energy in the first 100 iterations is shown in the upper part of Table 1 when $N = 1000$. We observe that E_n increases monotonically towards E_c . A quantitative fitting shows that $|E_n - E_c| \approx O(n^{-2}) + e_N$, where e_N is the difference of the limit of E_n , denoted by E_N^* , and E_c . The error e_N is mainly determined by the spatial resolution N , which is also shown in Table 1. A fitting shows that $|E_N^* - E_c| \approx O(h^{2.314})$. This suggests approximately second order convergence of the energy parameter with second order spatial discretization. We will leave the rigorous convergence analysis to the future study.

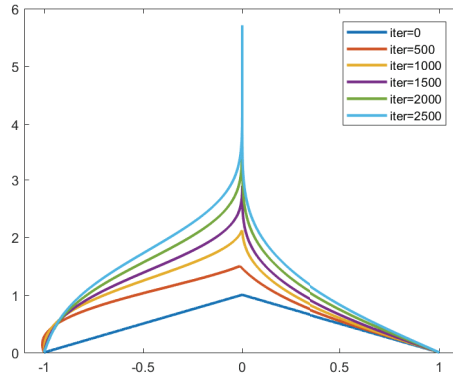
From Eq. (6.3) we have

$$U(0, y) = \left(\varepsilon\beta - \frac{1}{2}\right)y^2,$$

which shows that $U(x, y)$ is unbound along the y -axis when $\varepsilon\beta > \frac{1}{2}$. This violates the Assumption 2.2. In

Table 1 Upper part: Convergence of energy parameter with respect to the iteration number n . Lower part: Convergence of the limit energy with respect to the spatial resolution N .

IterNum n	10	20	30	50	100
$E_c - E_n$	2.1×10^{-3}	3.9×10^{-4}	1.5×10^{-4}	8.1×10^{-5}	6.2×10^{-5}
SpatialRes N	100	1000	2000	4000	5000
$E_c - E_N^*$	6.0×10^{-5}	2.0×10^{-5}	3.0×10^{-6}	1.2×10^{-7}	5.3×10^{-9}

**Figure 11** (Color Online). Divergence of the y -component of $\varphi^n(\alpha)$ in the iterations when $\varepsilon\beta > \frac{1}{2}$. Here we choose $\varepsilon = 1$, $\beta = 10$.

principle this is beyond our theoretical framework. But it is still interesting to apply EGMA in this case. Based on the result in Proposition 3.6, the energy parameter E will tend to infinity while the path may diverge along y -axis. The numerical results confirm this conjecture, although the current theory does not cover this case. The divergent curves are shown in Figure 11.

7 Conclusion and discussion

In this paper, we studied the minimization problem of the OM functional $S_T^{\text{OM}}[\psi]$ when T tends to infinity. Under mild conditions, we rigorously showed that the infimum of $S_T^{\text{OM}}[\psi]$ over ψ and T is always $-\infty$ and it occurs only when $T \rightarrow +\infty$. Moreover, we proved that when $T \rightarrow +\infty$, the minimizer of $S_T^{\text{OM}}[\psi]$ has convergent subsequence in the configuration space. With the help of Maupertuis principle, the problem of finding the graph limit of the minimizers of the OM functional is translated into that of finding an extremal of $\hat{S}_E[\varphi]$ with the energy $E^* = \max_{\mathbf{x}} U(\mathbf{x})$, where U is the path potential.

Based on these theoretical results, we designed an efficient algorithm (EGMA) to find the energy E^* and solve the Euler-Lagrange equation simultaneously. This algorithm can be viewed as a nontrivial extension of the geometric minimum action method (gMAM), which was proposed for the double minimization problem of the FW functional at zero temperature [22]. In gMAM, the energy E is fixed at zero, and the corresponding optimal transition time $T = \int_0^1 (2E - 2U(\varphi))^{-\frac{1}{2}} |\varphi'| \, d\alpha$ can be either finite or infinite. We note that the method can be extended to the case of non-zero E , which corresponds to a prescribed value for the transition time. In EGMA, the energy changes step by step to ensure that the time T always goes to infinity. This algorithm was successfully applied to several typical rare event examples. Although the rigorous proof of the convergence of the algorithm is still absent, our numerical examples in Sections 6.1 and 6.2 demonstrated that it converges to an extremal of $\hat{S}_{E^*}[\varphi]$ in practice.

Some possible extensions and unsolved problems arise naturally based on the theoretical analysis of the current paper. Below we list some of them.

- (i) As mentioned in the remarks, the conclusions that $\inf_T \inf_\psi S_T^{\text{OM}}[\psi] = -\infty$ and the minimizer of $S_T^{\text{OM}}[\psi]$ has convergent subsequence in the configuration space can be generalized to non-gradient systems with drift $\mathbf{b}(\mathbf{x})$ under suitable assumptions. However, the proof of the key result that φ^* is an extremal of $\hat{S}_{E^*}[\varphi]$ relies on the gradient form of $\mathbf{b}(\mathbf{x})$. Indeed, the proof of Lemma A.1 holds because the value of $\hat{S}_E[\varphi]$ is non-negative. Besides, we used an analog of Hartman-Grobman theorem to transfer the uniform BV property of φ'_k for linearized problem to the non-linear case in the neighborhood of the critical point \mathbf{x}_c . This approach requires that $(\mathbf{x}_c, 0)$ is a hyperbolic fixed point of the first order system (A.6). For non-gradient case, the first order system (A.6) becomes

$$\begin{aligned}\dot{\Psi}_1 &= \Psi_2, \\ \dot{\Psi}_2 &= -\nabla^2 U(\Psi_1) - (\nabla \mathbf{b}^T(\Psi_1) - \nabla \mathbf{b}(\Psi_1))\Psi_2.\end{aligned}\tag{7.1}$$

The point $(\mathbf{x}_c, 0)$ is still a fixed point. However, the eigenvalues of the Jacobian of (7.1) at $(\mathbf{x}_c, 0)$ have non-zero imaginary part. To study the behavior of φ'_k near the critical point, we might need more delicate study of the dynamics (7.1) on center manifold and more advanced result on linearization. So how to extend Theorem 3.10 to the non-gradient case remains an interesting issue.

- (ii) Presumably, the Freidlin-Wentzell functional can be viewed as a limit of Onsager-Machlup functional when $\varepsilon \rightarrow 0$. However, we have $\lim_{\varepsilon \rightarrow 0} \inf_T \inf_\psi S_T^{\text{OM}}[\psi] = -\infty$ by the Proposition 3.7. This suggests that a naive process is not valid to establish such connection. A possible alternative to investigate the limit of OM functional is to relate T and ε by a function $T = T(\varepsilon)$ and study the convergence of $\inf_\psi S_{T(\varepsilon)}^{\text{OM}}[\psi]$ as $\varepsilon \rightarrow 0$. This idea has been partially studied in [31]. They showed that for the scaling $T = \varepsilon^{-\alpha}$, $0 < \alpha \leq 1$, the OM functional Γ -converges to a functional completely characterized by the FW theory. However, for a more general and physical scaling $T = T(\varepsilon)$, the convergence of OM functional and its minimizer is not clear. The renormalized OM functional (1.9) might be a good candidate to perform such analysis.
- (iii) The discretization scheme described in EGMA can be further improved. For example, one may discretize $\hat{S}_E[\varphi]$ first then use some optimization methods like quasi-Newton or conjugate gradient type methods to search for the extremal. However, the algorithm we proposed here combines the iteration for solving Euler-Lagrange equation and finding the maximum of $U(\mathbf{x})$ simultaneously. It has the advantage that we can compute the optimal energy parameter and the MPP at the same time. This strategy may not apply for the optimization methods. Designing more efficient numerical methods to perform these two tasks together is an issue of practical interests.

In summary, the current work provides new ideas on the FW-OM dilemma. It will be instructive to further study the FW-OM connections with this new perspective.

Acknowledgements The authors are grateful to Profs. Shaobo Gan, Eric Vanden-Eijnden, Jiazhong Yang and Shulin Zhou for stimulating discussions. Special thanks are due to Prof. Wenmeng Zhang for his patient explanation about their recent progress on $C^{1,\beta}$ -linearization problem. The work of T. Li is supported by the NSFC under grants No. 11421101, 91530322 and 11825102. The work of W. Ren is partially supported by Singapore MOE ACRF grants R-146-000-267-114 (Tier-1) and R-146-000-232-112 (Tier-2), and NSFC grant No. 11871365. The work of X. Li is supported by the Construct Program of the Key Discipline in Hunan Province.

References

- 1 V.I. Arnold. *Mathematical methods of classical mechanics*. Springer-Verlag, Berlin, 1989.
- 2 A. Bovier, M. Eckhoff, V. Gaynard, and M. Klein. Metastability in reversible diffusion processes I. Sharp asymptotics for capacities and exit times. *J. Eur. Math. Soc.*, 6:399–424, 2004.
- 3 A. Bovier, V. Gaynard, and M. Klein. Metastability in reversible diffusion processes II. Precise asymptotics for small eigenvalues. *J. Eur. Math. Soc.*, 7:69–99, 2005.
- 4 M. Cameron, R.V. Kohn, and E. Vanden-Eijnden. The string method as a dynamical system. *J. Nonlinear Sci.*, 21:193–230, 2011.

- 5 G. Contreras, J. Delgado, and R. Iturriaga. Lagrangian flows: The dynamics of globally minimizing orbits-II. *Bull. Braz. Math. Soc.*, 28(2):155–196, 1997.
- 6 C.M. Dafermos. *Hyperbolic conservation laws in continuum physics*. Springer, Berlin and Heidelberg, 3rd edition, 2010.
- 7 C. Dellago, P.G. Bolhuis, and D. Chandler. Efficient transition path sampling: Application to Lennard-Jones cluster rearrangements. *J. Chem. Phys.*, 108(22):9236–9245, 1998.
- 8 M.M. Dunlop and A.M. Stuart. MAP estimators for piecewise continuous inversion. *Inverse. Probl.*, 32(10), 2016.
- 9 D. Dürr and A. Bach. The Onsager-Machlup function as Lagrangian for the most probable path of a diffusion process. *Commun. Math. Phys.*, 60(2):153–170, 1978.
- 10 W. E, W. Ren, and E. Vanden-Eijnden. String method for the study of rare events. *Phys. Rev. B*, 66(5):052301, 2002.
- 11 W. E, W. Ren, and E. Vanden-Eijnden. Minimum action method for the study of rare events. *Comm. Pure. Appl. Math.*, 57:637–656, 2004.
- 12 W. E, W. Ren, and E. Vanden-Eijnden. Simplified and improved string method for computing the minimum energy paths in barrier-crossing events. *J. Chem. Phys.*, 126(16):164103, 2007.
- 13 W. E and E. Vanden-Eijnden. Towards a theory of transition paths. *J. Stat. Phys.*, 123(3), 2006.
- 14 W. E and E. Vanden-Eijnden. Transition-path theory and path-finding algorithms for the study of rare events. *Ann. Rev. Phys. Chem.*, 61:391–420, 2010.
- 15 P. Faccioli, M. Sega, F. Pederiva, and H. Orland. Dominant pathways in protein folding. *Phys. Rev. Lett.*, 97(10):108101, 2006.
- 16 H. Fujisaki, M. Shiga, and A. Kidera. Onsager–Machlup action-based path sampling and its combination with replica exchange for diffusive and multiple pathways. *J. Chem. Phys.*, 132(13):134101, 2010.
- 17 H. Fujisaki, M. Shiga, K. Moritsugu, and A. Kidera. Multiscale enhanced path sampling based on the Onsager-Machlup action: Application to a model polymer. *J. Chem. Phys.*, 139(5):054117, 2013.
- 18 T. Fujita and S. Kotani. The Onsager-Machlup function for diffusion processes. *J. Math. Kyoto Univ.*, 22:115–130, 1982.
- 19 M. Giaquinta and S. Hildebrandt. *Calculus of variations I*. Springer Science & Business Media, Berlin, 2004.
- 20 R. Graham. Path integral formulation of general diffusion processes. *Z. Physik B*, 26:281–290, 1977.
- 21 P. Hänggi, P. Talkner, and M. Borkovec. Reaction-rate theory: Fifty years after Kramers. *Rev. Mod. Phys.*, 62:251–342, 1990.
- 22 M. Heymann and E. Vanden-Eijnden. The geometric minimum action method: A least action principle on the space of curves. *Comm. Pure. Appl. Math.*, 61(8):1052–1117, 2008.
- 23 N. Ikeda and S. Watanabe. *Stochastic differential equations and diffusion processes*. Wiley, New York, 1980.
- 24 L.D. Landau and E.M. Lifshitz. *Mechanics*, volume 1 of *Course of Theoretical Physics*. Butterworth-Heinemann, Oxford, 3rd edition, 1999.
- 25 J. Lee, I. Lee, I. Joung, J. Lee, and B.R. Brooks. Finding dominant reaction pathways via global optimization of action. *Biophys. J.*, 112(3):290a, 2017.
- 26 C. Lv, X. Li, F. Li, and T. Li. Constructing the energy landscape for genetic switching system driven by intrinsic noise. *PLoS One*, 9:e88167, 2014.
- 27 R.S. Maier and D.L. Stein. A scaling theory of bifurcations in the symmetric weak-noise escape problem. *J. Stat. Phys.*, 83(3-4):291–357, 1996.
- 28 R. Mané. Lagrangian flows: The dynamics of globally minimizing orbits. *Bull. Braz. Math. Soc.*, 28(2):141–153, 1997.
- 29 L. Onsager and S. Machlup. Fluctuations and irreversible processes. *Phys. Rev.*, 91(6):1505, 1953.
- 30 F.J. Pinski and A.M. Stuart. Transition paths in molecules at finite temperature. *J. Chem. Phys.*, 132(18):184104, 2010.
- 31 F.J. Pinski, A.M. Stuart, and F. Theil. Γ -limit for transition paths of maximal probability. *J. Stat. Phys.*, 146(5):955–974, 2012.
- 32 C. Schütte and M. Sarich. *Metastability and Markov state models in molecular dynamics: modeling, analysis, algorithmic approaches*, volume 24 of *Courant Lecture Notes*. Amer. Math. Soc., Providence, 2013.
- 33 Y. Takahashi and S. Watanabe. The probability functionals (Onsager-Machlup functions) of diffusion processes. In *Stochastic Integrals*, pages 433–463. Springer, 1981.
- 34 X. Wan. An adaptive high-order minimum action method. *J. Comp. Phys.*, 230:8669–8682, 2011.
- 35 J. Wang, K. Zhang, and E. Wang. Kinetic paths, time scale, and underlying landscapes: A path integral framework to study global natures of nonequilibrium systems and networks. *J. Chem. Phys.*, 133(12):125103, 2010.
- 36 O. Zeitouni. On the Onsager-Machlup functional of diffusion processes around non C^2 curves. *Ann. Prob.*, 17(3):1037–1054, 1989.
- 37 L. Zhang, W. Ren, A. Samanta, and Q. Du. Recent developments in computational modelling of nucleation in phase

transformations. *NPJ Comput. Mater.*, 2:16003, 2016.

- 38 W. Zhang, K. Lu, and W. Zhang. Differentiability of the conjugacy in the Hartman-Grobman theorem. *Trans. Amer. Math. Soc.*, 369:4995–5030, 2017.
- 39 P. Zhou and T. Li. Construction of the landscape for multi-stable systems: Potential landscape, quasi-potential, A-type integral and beyond. *J. Chem. Phys.*, 144(9):094109, 2016.
- 40 X. Zhou, W. Ren, and W. E. Adaptive minimum action method for the study of rare events. *J. Chem. Phys.*, 128(10):104111, 2008.

Appendix A Proof of Proposition 3.11

We now prove Proposition 3.11 in this Appendix. This relies on a series of lemmas. Some of them are quite technical. Recall that ψ_k is the minimizer of $S_{T_k}^{\text{OM}}[\psi]$, where $T_k \rightarrow +\infty$ as $k \rightarrow \infty$. The corresponding energy $E_k = E(T_k)$ and the extremal of $\hat{S}_{E_k}[\varphi]$ is φ_k for $k = 1, 2, \dots$. By theorem 3.9, we may assume $E_k \rightarrow E^*$ and $\varphi_k \rightarrow \varphi^*$ without loss of generality.

Our main idea is to show that each component of $\{\varphi'_k\}$ has uniformly bounded variations. Denote $\varphi_k'^{(i)}$ the i th component of φ'_k . We have the total variation

$$\begin{aligned} \int_0^1 \varphi_k'^{(i)}(\alpha) &= \sup_{\Delta} \sum_{j=0}^n |\varphi_k'^{(i)}(\alpha_{j+1}) - \varphi_k'^{(i)}(\alpha_j)| \\ &\leq \sup_{\Delta} \sum_{i=1}^d \sum_{j=0}^n |\varphi_k'^{(i)}(\alpha_{j+1}) - \varphi_k'^{(i)}(\alpha_j)| \\ &\leq \sup_{\Delta} \sum_{j=0}^n \sqrt{d} \left(\sum_{i=1}^d |\varphi_k'^{(i)}(\alpha_{j+1}) - \varphi_k'^{(i)}(\alpha_j)|^2 \right)^{\frac{1}{2}} \\ &= \sup_{\Delta} \sum_{j=0}^n \sqrt{d} |\varphi'_k(\alpha_{j+1}) - \varphi'_k(\alpha_j)|, \end{aligned} \tag{A.1}$$

where Δ is a partition of $[0, 1]$ with subdivision points $0 = \alpha_0 < \alpha_1 < \alpha_2 \cdots < \alpha_{n+1} = 1$. We only need to show that

$$\sup_{\Delta} \sum_{j=0}^n |\varphi'_k(\alpha_{j+1}) - \varphi'_k(\alpha_j)| \tag{A.2}$$

is uniformly bounded.

Next, we divide $[0, 1]$ into intervals in which $\varphi_k \in C^2$. We need the following lemma.

Lemma A.1. *There is a constant $K > 0$ which is independent of T , such that for any $T > 0$, $\#\{t \in [0, T] | U(\psi_T(t)) = E(T)\} \leq K$.*

Proof. By Assumption 2.3, we have the decomposition

$$\{\mathbf{x} | U(\mathbf{x}) = E(T)\} = \bigcup_{i=1}^N B_i,$$

where $B_i \cap B_j = \emptyset$ for $i \neq j$, B_i is closed and connected. We are going to show that ψ_T passes through each B_i at most once.

Assume that there exist $0 < t_1 < t_2 < T$ such that $\mathbf{x}_1 = \psi_T(t_1) \in B_i$, $\mathbf{x}_2 = \psi_T(t_2) \in B_i$. Define $\tilde{\psi}_{\tilde{T}}(t) = \psi_T(t+t_1)$ for $t \in [0, t_2-t_1]$, where $\tilde{T} = t_2-t_1$. $\tilde{\psi}_{\tilde{T}}$ must be the minimizer of $S_{\tilde{T}}[\psi]$ with boundary conditions $\psi(0) = \mathbf{x}_1$, $\psi(\tilde{T}) = \mathbf{x}_2$. Since $\tilde{\psi}_{\tilde{T}}$ is the minimizer of $S_{\tilde{T}}[\psi]$, by Maupertuis principle we know that the minimizer $\tilde{\psi}_{\tilde{T}}$ induces a geodesic on B_i from \mathbf{x}_1 to \mathbf{x}_2 with Riemannian metric [1](Theorem in page 246)

$$d\rho_E = \sqrt{2E(T) - U(\varphi)} |d\varphi|.$$

$\tilde{\psi}_T$ must lie on B_i since it minimizes the distance induced by ρ_E . However, we have

$$T \geq \int_{\mathbf{x}_1}^{\mathbf{x}_2} \frac{|\mathrm{d}\tilde{\psi}_T|}{\sqrt{2E(T) - 2U(\tilde{\psi}_T)}} = +\infty.$$

This contradiction implies that ψ_T passes through B_i at most once.

Since there are only finite components B_i of level set $\{\mathbf{x}|U(\mathbf{x}) = E(T)\}$, there is a positive lower bound of the distance between each two components

$$\min_{i \neq j} \text{dist}(B_i, B_j) = l > 0.$$

By Assumption 2.9, the length of ψ_T is uniformly bounded. So we have for any $T > 0$,

$$M \geq \int_0^T |\dot{\psi}_T| dt \geq (K-1)l.$$

This leads to the conclusion that K is finite and independent of T . \square

Lemma A.1 shows that for any k , the points α satisfying $U(\varphi_k(\alpha)) = E_k$ are finite. Note that when $U(\varphi_k(\alpha)) < E_k$, $\varphi_k \in C^2$. By Euler-Lagrange equation (3.14), in an interval $[\beta_1, \beta_2]$ such that $\varphi_k \in C^2$, the total variation of φ'_k is

$$\bigvee_{\beta_1}^{\beta_2} \varphi_k^{(i)} \leq \int_{\beta_1}^{\beta_2} |\varphi_k''| d\alpha = \int_{\beta_1}^{\beta_2} \frac{|\varphi_k'| \sqrt{|\nabla U|^2 |\varphi_k'|^2 - \langle \nabla U, \varphi_k' \rangle^2}}{2E_k - 2U(\varphi_k)} d\alpha. \quad (\text{A.3})$$

We can rewrite Eq. (A.3) with time parameterization as

$$\begin{aligned} \int_{\beta_1}^{\beta_2} |\varphi_k''| d\alpha &= \int_{\beta_1}^{\beta_2} \frac{|\varphi_k'| \sqrt{|\nabla U|^2 |\varphi_k'|^2 - \langle \nabla U, \varphi_k' \rangle^2}}{2E_k - 2U(\varphi_k)} d\alpha \\ &= \int_{\beta_1}^{\beta_2} \frac{|\varphi_k'|^2 \sqrt{|\nabla U|^2 |\hat{\tau}_k|^2 - \langle \nabla U, \hat{\tau}_k \rangle^2}}{2E_k - 2U(\varphi_k)} d\alpha \\ &= \int_{t_1}^{t_2} \frac{|\varphi_k'|^2 \sqrt{|\nabla U|^2 |\dot{\psi}_k|^2 - \langle \nabla U, \dot{\psi}_k \rangle^2}}{|\dot{\psi}_k|^3} \frac{d\alpha}{dt} dt \\ &= |\varphi_k'| \int_{t_1}^{t_2} \sqrt{\frac{|\nabla U|^2 |\dot{\psi}_k|^2 - \langle \nabla U, \dot{\psi}_k \rangle^2}{|\dot{\psi}_k|^4}} dt, \end{aligned} \quad (\text{A.4})$$

where $\hat{\tau}_k = \varphi_k'/|\varphi_k'|$, $t_1 = \ell^{-1}(\beta_1)$ and $t_2 = \ell^{-1}(\beta_2)$.

For any $T > 0$, we define

$$\Theta_T(t) = \frac{|\nabla U(\psi_T)|^2 |\dot{\psi}_T|^2 - \langle \nabla U(\psi_T), \dot{\psi}_T \rangle^2}{|\dot{\psi}_T|^4} \quad (\text{A.5})$$

and denote $\Theta_k(t) = \Theta_{T_k}(t)$. It is obvious that $\Theta_T(t)$ is well-defined for $U(\psi_T(t)) < E(T)$. Recall that the minimizer ψ_T satisfies the Euler-Lagrange equation

$$\ddot{\psi} + \nabla U(\psi) = 0,$$

or equivalently the first order system

$$\begin{aligned} \dot{\Psi}_1 &= \Psi_2, \\ \dot{\Psi}_2 &= -\nabla U(\Psi_1). \end{aligned} \quad (\text{A.6})$$

We have $\psi \equiv \Psi_1$. We will use $\tilde{\Psi}$ to denote the extended variable $(\Psi_1, \Psi_2) \in \mathbb{R}^{2d}$. The state $\tilde{\Psi}_c = (\mathbf{x}_c, 0)$ is a fixed point of the system, where \mathbf{x}_c is a critical point. The following lemma shows that the function $\Theta_T(t)$ can be continuously extended to $t \in [0, T]$.

Lemma A.2 (Preliminary properties of Θ_T and Ψ). (1) Given $\mathbf{x}_s \neq \mathbf{x}_c$, $\mathbf{x}_f \neq \mathbf{x}_c$ and $T > 0$, $\lim_{s \rightarrow t} \Theta_T(s)$ exists for any $t \in [0, T]$.

(2) There exists a neighborhood \mathcal{U} of critical point \mathbf{x}_c and constant $m > 0$, such that for any given $t_0 > 0$, $\mathbf{x}_s, \mathbf{x}_f \in \partial\mathcal{U}$, we have $|\Psi_2| \geq m > 0$ for $t \in [0, t_0]$ when $T \rightarrow +\infty$.

Proof. (1) Since $\Psi_1, \Psi_2 \in C^1[0, T]$, Θ_T is continuous except the points with $\Psi_2(t_c) = 0$. Below we will show these points are removable singularities.

Suppose $\Psi_2(t_c) = 0$. We have the following Taylor expansion near t_c

$$\begin{aligned} -\nabla U(\Psi_1) &= \Psi^{(2)} + \frac{1}{2}\Psi^{(4)}(t-t_c)^2 + \frac{1}{24}\Psi^{(6)}(t-t_c)^4 + o(t-t_c)^5, \\ \Psi_2 &= \Psi^{(2)}(t-t_c) + \frac{1}{6}\Psi^{(4)}(t-t_c)^3 + \frac{1}{120}\Psi^{(6)}(t-t_c)^5 + o(t-t_c)^6, \end{aligned} \tag{A.7}$$

where $\Psi^{(2)}, \Psi^{(4)}, \Psi^{(6)}$ are corresponding higher derivatives of $\Psi_1(t)$ assuming value at t_c . The odd order derivatives of Ψ_1 disappear because $\Psi^{(1)} = 0$,

$$\Psi^{(3)} = \frac{d}{dt}\Psi_1^{(2)} = -\frac{d}{dt}\nabla U(\Psi_1) = -\nabla^2 U \cdot \dot{\Psi}_1 = 0$$

and

$$\Psi^{(5)} = \frac{d}{dt}\Psi_1^{(4)} = \frac{d}{dt}\nabla^2 U \nabla U = \nabla(\nabla^2 U \nabla U) \cdot \dot{\Psi}_1 = 0.$$

Substituting (A.7) into $\Theta_T(t)$, we obtain that in a neighborhood of t_c ,

$$\Theta_T(t) = \frac{(|\Psi^{(2)}|^2 |\Psi^{(4)}|^2 - \langle \Psi^{(2)}, \Psi^{(4)} \rangle^2)(t-t_c)^2 + o(t-t_c)^2}{9|\Psi^{(4)}|^2 + o(1)}. \tag{A.8}$$

With the fact that $\Psi^{(2)} = -\nabla U$, $\Psi^{(4)} = \nabla^2 U \nabla U$ taking value at $\Psi_1(t_c)$, we have

$$\Theta_T(t) = \frac{[\widehat{\nabla U}(\nabla^2 U)^2 \widehat{\nabla U} - (\widehat{\nabla U} \nabla^2 U \widehat{\nabla U})^2](t-t_c)^2 + o(t-t_c)^2}{9 + o(1)},$$

where $\widehat{\nabla U} = \nabla U / |\nabla U|$. Since Ψ_1 is uniformly bounded, $\lim_{t \rightarrow t_c} \Theta_T(t) = 0$. This ends the proof of the first statement.

(2) By assumption 2.6, all eigenvalues of $\nabla^2 U(\mathbf{x}_c)$ are negative, so there is a neighborhood \mathcal{U} of \mathbf{x}_c , for any $\mathbf{x} \in \partial\mathcal{U}$, $\mathbf{x} \neq \mathbf{x}_c$, $U(\mathbf{x}) < U(\mathbf{x}_c)$. For $\mathbf{x}, \mathbf{y} \in \mathbb{R}^d$, let $(\Phi_1(t, \mathbf{x}, \mathbf{y}), \Phi_2(t, \mathbf{x}, \mathbf{y}))$ be the solution of (A.6) at time t with initial condition $\Psi_1(0) = \mathbf{x}$, $\Psi_2(0) = \mathbf{y}$. So $\Psi_1(t) = \Phi_1(t, \mathbf{x}_s, \mathbf{y}_s(T))$, $\Psi_2(t) = \Phi_2(t, \mathbf{x}_s, \mathbf{y}_s(T))$ for some proper \mathbf{y}_s . Conservation of energy implies

$$|\mathbf{y}_s|^2 = 2E(T) - 2U(\mathbf{x}_s). \tag{A.9}$$

From $E(T) \rightarrow E^*$, \mathbf{x}_s assumes value on a compact set $\partial\mathcal{U}$, we know $|\mathbf{y}_s|^2 \leq 2(E^* + 1) + 2 \max_{\mathbf{x}_s \in \partial\mathcal{U}} U(\mathbf{x}_s)$ for large enough T .

Because $\Phi_1(t, \mathbf{x}, \mathbf{y}), \Phi_2(t, \mathbf{x}, \mathbf{y})$ are continuous functions of $(t, \mathbf{x}, \mathbf{y})$, the triple $(t, \mathbf{x}, \mathbf{y})$ assumes value in a compact set $[0, t_0] \times \partial\mathcal{U} \times \{|\mathbf{y}| \leq 2(E^* + 1) + 2 \max_{\mathbf{x}_s \in \partial\mathcal{U}} U(\mathbf{x}_s)\}$, the continuous function $|\Phi_1 - \mathbf{x}_c|^2 + |\Phi_2|^2$ has a minimum m . Note that $(\mathbf{x}_c, 0)$ is a fixed point of (A.6), the minimum m must be positive, otherwise the uniqueness of initial value problem will be violated. So we have

$$|\Phi_1(t, \mathbf{x}_s, \mathbf{y}_s) - \mathbf{x}_c|^2 + |\Phi_2(t, \mathbf{x}_s, \mathbf{y}_s)|^2 \geq m > 0. \tag{A.10}$$

Let $t_m(T) = \arg \min_{t \in [0, t_0]} |\Phi_2(t, \mathbf{x}_s, \mathbf{y}_s(T))|$, we have

$$\liminf_{T \rightarrow +\infty} |\Phi_2(t_m(T), \mathbf{x}_s, \mathbf{y}_s(T))| > 0. \tag{A.11}$$

Otherwise, there is a subsequence T_k such that $|\Phi_2(t_m(T_k), \mathbf{x}_s, \mathbf{y}_s(T_k))| \rightarrow 0$. By the energy conservation (3.4), we get

$$\begin{aligned} \liminf_{k \rightarrow \infty} 2E(T_k) &= 2E^* = 2U(\mathbf{x}_c) \\ &= \liminf_{k \rightarrow \infty} \left\{ |\Phi_2(t_m, \mathbf{x}_s, \mathbf{y}_s(T_k))|^2 + 2U(\Phi_1(t_m(T_k), \mathbf{x}_s, \mathbf{y}_s(T_k))) \right\} \\ &= 2 \liminf_{k \rightarrow \infty} U(\Phi_1(t_m(T_k), \mathbf{x}_s, \mathbf{y}_s(T_k))). \end{aligned}$$

So we can select a subsequence $U(\Phi_1(t_m(T_{k_l}), \mathbf{x}_s, \mathbf{y}_s(T_{k_l})))$ such that

$$\lim_{l \rightarrow \infty} U(\Phi_1(t_m(T_{k_l}), \mathbf{x}_s, \mathbf{y}_s(T_{k_l}))) = U(\mathbf{x}_c).$$

Since the set $\{\Phi_1(t_m(T_{k_l}), \mathbf{x}_s, \mathbf{y}_s(T_{k_l}))\}$ is bounded, we can select a subsequence from $\Phi_1(t_m(T_{k_l}), \mathbf{x}_s, \mathbf{y}_s(T_{k_l}))$ which converges to a point \mathbf{x}_m . For simplicity, we still denote it by $\Phi_1(t_m(T_{k_l}), \mathbf{x}_s, \mathbf{y}_s(T_{k_l}))$. By continuity, $U(\mathbf{x}_c) = U(\mathbf{x}_m)$. Because \mathbf{x}_c is the unique maximum of $U(\mathbf{x})$ in \mathcal{U} , we must have $\mathbf{x}_m = \mathbf{x}_c$.

However, we know from (A.10) that

$$0 = \liminf_{l \rightarrow \infty} |\Phi_1(t_m(T_{k_l}), \mathbf{x}_s, \mathbf{y}_s(T_{k_l})) - \mathbf{x}_c|^2 + |\Phi_2(t_m(T_{k_l}), \mathbf{x}_s, \mathbf{y}_s(T_{k_l}))|^2 \geq m > 0.$$

This contradiction implies that (A.11) is true. So we have

$$|\Phi_2(t, \mathbf{x}_s, \mathbf{y}_s)| \geq |\Phi_2(t_m, \mathbf{x}_s, \mathbf{y}_s)| \geq m > 0.$$

The proof is completed. \square

With the help of Lemmas A.1 and A.2, we can show that for any fixed k , φ'_k has bounded variation.

Lemma A.3. *For fixed $T_k > 0$, φ'_k has bounded variation.*

Proof. It is sufficient to show

$$\sup_{\Delta} \sum_{j=0}^n |\varphi'_k(\alpha_{j+1}) - \varphi'_k(\alpha_j)| \tag{A.12}$$

is bounded, where Δ is a partition of $[0, 1]$, i.e.,

$$\Delta : 0 = \alpha_0 < \alpha_1 < \alpha_2 < \dots < \alpha_{n+1} = 1.$$

By Lemma A.1, the set $\{\alpha \in [0, 1] | U(\varphi_k(\alpha)) = E_k\}$ is finite. Denote the elements in this set by $\alpha_1^k < \alpha_2^k < \dots < \alpha_N^k$. The summation in (A.12) can be divided into two cases.

Case I: $\alpha_j \in (\alpha_i^k, \alpha_{i+1}^k)$ for some $0 \leq i \leq N-1$ and $\alpha_{j+1} \notin (\alpha_i^k, \alpha_{i+1}^k)$. Denote the index set for j in this case by I.

By Lemma A.1, $\#\{j \in \text{I}\} \leq N$. We have

$$\sum_{j \in \text{I}} |\varphi'_k(\alpha_{j+1}) - \varphi'_k(\alpha_j)| \leq 2NM. \tag{A.13}$$

Case II: $\alpha_j, \alpha_{j+1} \in (\alpha_i^k, \alpha_{i+1}^k)$. Denote the index set for j in this case by II.

For $j \in \text{II}$, $\varphi_k \in C^2[\alpha_j, \alpha_{j+1}]$. We have

$$\begin{aligned} \sum_{j \in \text{II}} |\varphi'_k(\alpha_{j+1}) - \varphi'_k(\alpha_j)| &= \sum_{j \in \text{II}} \left| \int_{\alpha_j}^{\alpha_{j+1}} \varphi''_k \, d\alpha \right| \\ &\leq \sum_{l=1}^N \int_{\alpha_l^k}^{\alpha_{l+1}^k} |\varphi''_k| \, d\alpha \\ &\leq \sum_{l=1}^N \int_{t_l^k}^{t_{l+1}^k} \sqrt{\Theta_k(t)} \, dt \\ &= \int_0^{T_k} \sqrt{\Theta_k(t)} \, dt, \end{aligned}$$

where $t_l^k = \ell_k^{-1}(\alpha_l^k)$. ℓ_k is defined in (3.34). By Lemma A.2, $\Theta(t)$ is continuous so it is bounded by M_Θ in $[0, T_k]$. This leads to

$$\sum_{j \in \mathbb{I}} |\varphi'_k(\alpha_{j+1}) - \varphi'_k(\alpha_j)| \leq \sqrt{M_\Theta T_k}.$$

Combining with (A.13), φ'_k has bounded variation. □

By Proposition 3.9, we know that φ_k , which has the same graph as ψ_k , tends to φ^* passing through a critical point \mathbf{x}_c when $T \rightarrow \infty$. We will show that φ'_k has uniformly bounded variation in a neighborhood of \mathbf{x}_c . This will be done through linearization analysis and Hartman-Grobman theorem.

In the neighborhood of $(\mathbf{x}_c, 0)$, The nonlinear system (A.6) can be well-approximated by its linearizaion

$$\begin{aligned} \dot{\mathbf{x}}_1 &= \mathbf{x}_2, \\ \dot{\mathbf{x}}_2 &= A^2 \mathbf{x}_1, \end{aligned} \tag{A.14}$$

where $A^2 = -\nabla^2 U(\mathbf{x}_c)$. Because all eigenvalues of $\nabla^2 U(\mathbf{x}_c)$ are negative, we may denote the eigenvalues of A by $0 < \mu_1 \leq \mu_2 \leq \dots \leq \mu_d$, the corresponding unit orthogonal eigenvectors by $\xi_1, \xi_2, \dots, \xi_d$. We also use $\tilde{\mathbf{x}}$ to denote the extended variable $\tilde{\mathbf{x}} = (\mathbf{x}_1, \mathbf{x}_2)$. For the linearized system (A.14), we have the following lemma.

Lemma A.4. *The solution of (A.14) with boundary condition $\mathbf{x}_1(0) = \mathbf{x}_s, \mathbf{x}_1(T) = \mathbf{x}_f$ is*

$$\begin{aligned} \mathbf{x}_1(t) &= (e^{AT} - e^{-AT})^{-1} [e^{At}(\mathbf{x}_f - e^{-AT} \mathbf{x}_s) + e^{A(T-t)}(\mathbf{x}_s - e^{-AT} \mathbf{x}_f)], \\ \mathbf{x}_2(t) &= (e^{AT} - e^{-AT})^{-1} A [e^{At}(\mathbf{x}_f - e^{-AT} \mathbf{x}_s) - e^{A(T-t)}(\mathbf{x}_s - e^{-AT} \mathbf{x}_f)]. \end{aligned} \tag{A.15}$$

For any $\mathbf{x}_s \neq 0, \mathbf{x}_f \neq 0, \mathbf{x}_s \neq \mathbf{x}_f$, the integral

$$\int_0^T \sqrt{\Theta_T^L(t)} dt$$

is uniformly bounded with respect to T , where

$$\Theta_T^L(t) = \frac{(\mathbf{x}_1^T A^4 \mathbf{x}_1) |\mathbf{x}_2|^2 - (\mathbf{x}_1^T A^2 \mathbf{x}_2)^2}{|\mathbf{x}_2|^4} \tag{A.16}$$

Proof. It is straightforward to check that (A.15) is the solution of the boundary value problem. The function $\Theta_T^L(t)$ is a special case of $\Theta_T(t)$ defined in (A.5) by taking $U(\mathbf{x}) = -\mathbf{x}^T A^2 \mathbf{x}$. By Lemma A.2, we only need to consider the case that T is sufficiently large. For simplicity, we denote $\Theta_T^L(t) = F(t)/|\mathbf{x}_2|^4$, where

$$F(t) = (\mathbf{x}_1^T A^4 \mathbf{x}_1) |\mathbf{x}_2|^2 - (\mathbf{x}_1^T A^2 \mathbf{x}_2)^2. \tag{A.17}$$

Denote $\mathbf{x}_s^i = \mathbf{x}_s^T \xi_i, \mathbf{x}_f^i = \mathbf{x}_f^T \xi_i, i = 1, 2, \dots, d$. We have explicit form of $F(t)$ and $|\mathbf{x}_2|^2$

$$\begin{aligned} F(t) &= \sum_{i < j} \left\{ \mu_i^2 \mu_j (e^{\mu_i T} - e^{-\mu_i T})^{-1} (e^{\mu_j T} - e^{-\mu_j T})^{-1} [p_i e^{\mu_i t} + q_i e^{\mu_i (T-t)}] \right. \\ &\quad [p_j e^{\mu_j t} - q_j e^{\mu_j (T-t)}] - \mu_i \mu_j^2 (e^{\mu_i T} - e^{-\mu_i T})^{-1} (e^{\mu_j T} - e^{-\mu_j T})^{-1} \\ &\quad \left. [p_i e^{\mu_i t} - q_i e^{\mu_i (T-t)}] [p_j e^{\mu_j t} + q_j e^{\mu_j (T-t)}] \right\}^2 \\ &=: \sum_{i < j} f_{ij}^2(t), \\ |\mathbf{x}_2|^2 &= \sum_i \mu_i^2 (e^{\mu_i T} - e^{-\mu_i T})^{-2} [p_i e^{\mu_i t} - q_i e^{\mu_i (T-t)}]^2, \end{aligned}$$

where $p_i = \mathbf{x}_f^i - e^{-\mu_i T} \mathbf{x}_s^i, q_i = \mathbf{x}_s^i - e^{-\mu_i T} \mathbf{x}_f^i$. Clearly, if $\mathbf{x}_s^i, \mathbf{x}_f^i \neq 0$, when T gets large enough, $p_i, q_i \neq 0$ and they are uniformly bounded.

We first show that in $[0, T/2]$, $\int_0^{T/2} \sqrt{\Theta_T^L(t)} dt$ is uniformly bounded. We have

$$\sqrt{\Theta_T^L(t)} = \frac{\sqrt{\sum_{i < j} f_{ij}^2}}{|\mathbf{x}_2|^2} \leq C \frac{\max_{i < j} |f_{ij}|}{|\mathbf{x}_2|^2} \leq C \sum_{i < j} \frac{|f_{ij}|}{|\mathbf{x}_2|^2}.$$

It is sufficient to show for each pair $i < j$,

$$\int_0^{T/2} \frac{|f_{ij}|}{|\mathbf{x}_2|^2} dt$$

is uniformly bounded.

The key idea of the proof is to verify that f_{ij} and $|\mathbf{x}_2|^2$ can be dominated by an exponential function. For given \mathbf{x}_s , let us denote the sets

$$S = \{i | x_s^i \neq 0\}, \quad \bar{S} = \{1, 2, \dots, d\} \setminus S.$$

Since $\mathbf{x}_s \neq 0$, S is not empty. For different choices of \mathbf{x}_s and \mathbf{x}_f , we divide the proof into 4 cases.

Case 1: $i, j \in \bar{S}, i \neq j$.

If \bar{S} is not empty, for every $i \in \bar{S}$, we can always assume $x_f^i \neq 0$. Otherwise $f_{ij} = 0$ for any j . If $\mu_i = \mu_j$, $f_{ij} = 0$. For $\mu_i < \mu_j$

$$|f_{ij}| \leq C e^{(\mu_i + \mu_j)(t-T)},$$

where C is a generic positive constant independent of T . At the same time,

$$|\mathbf{x}_2|^2 \geq C e^{2\mu_i(t-T)}.$$

Thus

$$\begin{aligned} \int_0^{T/2} \frac{|f_{ij}|}{|\mathbf{x}_2|^2} dt &\leq C \int_0^{T/2} e^{(\mu_j - \mu_i)(t-T)} dt \\ &= \frac{C}{\mu_j - \mu_i} (e^{-\frac{1}{2}(\mu_j - \mu_i)T} - e^{-(\mu_j - \mu_i)T}) \leq \frac{2C}{\mu_j - \mu_i}, \end{aligned} \quad (\text{A.18})$$

which is uniformly bounded.

Case 2.1: $i \neq j \in S, \mu_i < \mu_j$.

In this case, f_{ij} can be bounded by an exponential function

$$|f_{ij}| \leq C e^{-(\mu_i + \mu_j)t}. \quad (\text{A.19})$$

The denominator $|\mathbf{x}_2|^2$ can be estimated by

$$|\mathbf{x}_2|^2 \geq \mu_i^2 [p_i e^{\mu_i(2t-T)} - q_i]^2 e^{-2\mu_i t} + \mu_j^2 [p_j e^{\mu_j(2t-T)} - q_j]^2 e^{-2\mu_j t}. \quad (\text{A.20})$$

If for every $t \in [0, T/2]$, $(p_i e^{\mu_i(2t-T)} - q_i)^2 > 0$, there is a positive lower bounded such that

$$|\mathbf{x}_2|^2 \geq C e^{-2\mu_i t}.$$

We have

$$\begin{aligned} \int_0^{T/2} \frac{|f_{ij}|}{|\mathbf{x}_2|^2} dt &\leq C \int_0^{T/2} e^{-(\mu_j - \mu_i)t} dt \\ &= \frac{C}{\mu_j - \mu_i} (1 - e^{-\frac{1}{2}(\mu_j - \mu_i)T}) \leq \frac{C}{\mu_j - \mu_i}. \end{aligned} \quad (\text{A.21})$$

If there is a $t_i \in [0, T/2]$ such that $p_i e^{\mu_i t_i} - q_i e^{\mu_i(T-t_i)} = 0$, then we define $\rho_i = (q_i/p_i)^{\frac{1}{\mu_i}}$, $\rho_j = (q_j/p_j)^{\frac{1}{\mu_j}}$ if $p_j q_j > 0$. The constants ρ_i, ρ_j are uniformly bounded with respect to T . We have $e^{2t_i} = \rho_i e^T$. We will show that in a neighborhood of t_i , the integral is uniformly bounded.

If $\rho_i = \rho_j = \rho$, we can obtain the estimation

$$|f_{ij}| \leq 4\mu_i\mu_j |p_i| |p_j| \rho^{\frac{1}{2}(\mu_i+\mu_j)} (\mu_j - \mu_i)(t - t_i)^2 e^{-\frac{1}{2}(\mu_j+\mu_i)T} + o(t - t_i)^2 e^{-\frac{1}{2}(\mu_j+\mu_i)T}. \tag{A.22}$$

The denominator

$$|\mathbf{x}_2|^2 \geq C(t - t_i)^2 e^{-2\mu_i T} + o(t - t_i)^2 e^{-2\mu_i T}. \tag{A.23}$$

So there is a $\delta > 0$ independent of T , in $[t_i - \delta, t_i + \delta]$,

$$\frac{|f_{ij}|}{|\mathbf{x}_2|^2} \leq \frac{(C + o(1))e^{-\frac{1}{2}(\mu_j-\mu_i)T}}{C + o(1)} \leq 1.$$

The integration $\int_{t_i-\delta}^{t_i+\delta} |f_{ij}|/|\mathbf{x}_2|^2 dt$ is uniformly bounded.

If $\rho_i \neq \rho_j$, there is a neighborhood of t_i such that $(p_j e^{\mu_j(2t-T)} - q_j)^2 > 0$. With Taylor expansion near t_i , we obtain

$$|f_{ij}| \leq C e^{-\frac{1}{2}(\mu_i+\mu_j)T}. \tag{A.24}$$

$$|\mathbf{x}_2|^2 \geq (C^2 + o(1))(t - t_i)^2 e^{-\mu_i T} + e^{-\mu_j T}. \tag{A.25}$$

So there is a $\delta > 0$ such that in $[t_i - \delta, t_i + \delta]$,

$$|\mathbf{x}_2|^2 \geq C(t - t_i)^2 e^{-\mu_i T} + C e^{-\mu_j T}.$$

In all, the integration

$$\begin{aligned} \int_{t_i-\delta}^{t_i+\delta} \frac{|f_{ij}|}{|\mathbf{x}_2|^2} dt &\leq C \int_{t_i-\delta}^{t_i+\delta} \frac{e^{-\frac{1}{2}(\mu_j-\mu_i)T}}{C^2(t - t_i)^2 + e^{-(\mu_j-\mu_i)T}} dt \\ &= 2 \int_0^\delta \frac{C de^{\frac{1}{2}(\mu_j-\mu_i)T} s}{1 + (Ce^{\frac{1}{2}(\mu_j-\mu_i)T} s)^2} dt \\ &= C \int_0^{C\delta e^{\frac{1}{2}(\mu_j-\mu_i)T}} \frac{ds}{1 + s^2} \leq C \frac{\pi}{2} \end{aligned} \tag{A.26}$$

is uniformly bounded.

To summarize, we have shown that there exists a $\delta > 0$, the integration in the neighborhood $[t_i - \delta, t_i + \delta]$ is uniformly bounded. Outside this interval, we have

$$|\mathbf{x}_2|^2 \geq C e^{-2\mu_i t}.$$

Thus

$$\begin{aligned} \int_0^{T/2} \frac{|f_{ij}|}{|\mathbf{x}_2|^2} dt &= \int_0^{t_i-\delta} + \int_{t_i-\delta}^{t_i+\delta} + \int_{t_i+\delta}^{T/2} \frac{|f_{ij}|}{|\mathbf{x}_2|^2} dt \\ &\leq C + \int_0^{T/2} e^{-(\mu_j-\mu_i)t} dt \leq C + \frac{1}{\mu_j - \mu_i}. \end{aligned} \tag{A.27}$$

Case 2.2: $i \neq j \in S$, $\mu_i = \mu_j = \mu$.

The proof in this case is similar as Case 2.1. The main difference is that the estimation of $|f_{ij}|$ is replaced by

$$|f_{ij}| \leq C e^{-\mu T}. \tag{A.28}$$

If there exists t_i such that $p_i e^{\mu t_i} - q_i e^{\mu(T-t_i)} = 0$, the estimation (A.22), (A.23), (A.24) and (A.25) imply that $|f_{ij}|/|\mathbf{x}_2|^2$ is uniformly bounded in $[t_i - \delta, t_i + \delta]$. Outside this interval,

$$|\mathbf{x}_2|^2 \geq C e^{-2\mu t}.$$

Thus

$$\begin{aligned} \int_0^{T/2} \frac{|f_{ij}|}{|\mathbf{x}_2|^2} dt &= \int_0^{t_i-\delta} + \int_{t_i-\delta}^{t_i+\delta} + \int_{t_i+\delta}^{T/2} \frac{|f_{ij}|}{|\mathbf{x}_2|^2} dt \\ &\leq C + e^{-\mu T} \int_0^{T/2} e^{2\mu t} dt \leq C + \frac{1}{\mu}. \end{aligned} \tag{A.29}$$

Case 3: $i \in S, j \in \bar{S}$.

In this case, we can estimate f_{ij} and $|\mathbf{x}_2|^2$ by

$$\begin{aligned} |f_{ij}| &\leq \left| \mu_i x_f^i [p_i e^{\mu_i(2t-T)} + q_i] [e^{\mu_j t} - e^{-\mu_j t}] - \mu_j x_f^j [p_i e^{\mu_i(2t-T)} - q_i] [e^{\mu_j t} + e^{-\mu_j t}] \right| \\ &\leq C e^{-\mu_i t} e^{-\mu_j T} \leq C e^{-\mu_i t} e^{\mu_j(t-T)}. \\ |\mathbf{x}_2|^2 &\geq \mu_i^2 [p_i e^{\mu_i(2t-T)} - q_i]^2 e^{-2\mu_i t} + \mu_j^2 |x_f^j|^2 (e^{\mu_j t} + e^{-\mu_j t})^2 e^{-2\mu_j T}. \end{aligned} \quad (\text{A.30})$$

If there exists $t_i \in [0, T/2]$ such that $p_i e^{\mu_i(2t-T)} - q_i = 0$, we can take similar argument as in Case 2.1. So in a δ -neighborhood of t_i , the integration is uniformly bounded. Outside this neighborhood, we have

$$|\mathbf{x}_2|^2 \geq C(e^{-2\mu_i t} + e^{2\mu_j(t-T)}).$$

Since $\mu_j \geq \mu_i$, $t \leq T/2$, we have $e^{-2\mu_i t} \geq e^{2\mu_j(t-T)}$. Thus

$$\begin{aligned} \int_0^{T/2} \frac{|f_{ij}|}{|\mathbf{x}_2|^2} dt &= \int_0^{t_i-\delta} + \int_{t_i-\delta}^{t_i+\delta} + \int_{t_i+\delta}^{T/2} \frac{|f_{ij}|}{|\mathbf{x}_2|^2} dt \\ &\leq C + C \int_0^{T/2} e^{(\mu_i+\mu_j)t} e^{-\mu_j T} dt \\ &\leq C + \frac{C}{\mu_i + \mu_j} (e^{-(\mu_j-\mu_i)T} - e^{-\mu_j T}) \\ &\leq C + \frac{2C}{\mu_i + \mu_j}. \end{aligned} \quad (\text{A.31})$$

Case 4: $i \in \bar{S}, j \in S$.

As in Case 3, we have

$$|f_{ij}| \leq C e^{-\mu_j t} e^{\mu_i(t-T)}, \quad (\text{A.32})$$

$$|\mathbf{x}_2|^2 \geq \mu_j^2 [p_j e^{\mu_j(2t-T)} - q_j]^2 e^{-2\mu_j t} + \mu_i^2 |x_f^i|^2 (e^{\mu_i t} + e^{-\mu_i t})^2 e^{-2\mu_i T}. \quad (\text{A.33})$$

If there exists a $t_j \in [0, T/2]$ such that $p_j e^{\mu_j(2t-T)} - q_j = 0$, similar argument as the Case 2.1 holds. We have boundedness of the integrand in a δ -neighborhood of t_j , and

$$|\mathbf{x}_2|^2 \geq C(e^{-2\mu_j t} + e^{2\mu_i(t-T)})$$

outside the δ -neighborhood.

Denote $t_c = \frac{\mu_i T}{\mu_i + \mu_j}$. When $t \leq t_c$, $e^{-2\mu_j t} \geq e^{2\mu_i(t-T)}$. When $t \geq t_c$, $e^{-2\mu_j t} \leq e^{2\mu_i(t-T)}$. So we have the estimate

$$\begin{aligned} \int_0^{T/2} \frac{|f_{ij}|}{|\mathbf{x}_2|^2} dt &\leq \int_{t_j-\delta}^{t_j+\delta} \frac{|f_{ij}|}{|\mathbf{x}_2|^2} dt + C \int_0^{t_c} e^{(\mu_i+\mu_j)t} e^{-\mu_i T} dt + C \int_{t_c}^{T/2} e^{-\mu_j t} e^{-\mu_i(t-T)} dt \\ &\leq C + \frac{C}{\mu_i + \mu_j} e^{-\mu_i T} (e^{\mu_i T} - 1) + \frac{C}{\mu_i + \mu_j} e^{\mu_i T} (e^{-\mu_i T} - e^{-\frac{1}{2}(\mu_i+\mu_j)T}) \\ &\leq C + \frac{C}{\mu_i + \mu_j}. \end{aligned}$$

So far, we have shown that $\int_0^{T/2} \sqrt{\Theta_T^L(t)} dt$ is uniformly bounded. As for the interval $[T/2, T]$, we can define $s = T - t$, repeat previous discussions to show that $\int_{T/2}^T \sqrt{\Theta_T^L(t)} dt$ is also uniformly bounded. The proof is done. \square

In order to show the uniformly bounded variation of φ'_k in the neighborhood of a critical point \mathbf{x}_c , we employ a strengthened version of Hartman-Grobman theorem to control the nonlinearity[38]. Let $T^t(\tilde{\mathbf{x}}_0)$, $L^t(\tilde{\mathbf{x}}_0)$ be the solution of the nonlinear system (A.6) or the linear system (A.14), respectively, at time t with the initial condition $\tilde{\Psi}(0) = \tilde{\mathbf{x}}_0$ or $\tilde{\mathbf{x}}(0) = \tilde{\mathbf{x}}_0$.

Lemma A.5. *There exists a neighborhood \mathcal{U} of $\tilde{\Psi}_c$ and a homeomorphism $H : \mathcal{U} \rightarrow \mathbb{R}^{2d}$ such that $HT^t = L^tH$ for any $t > 0$ and*

$$H(\tilde{\Psi}) = \tilde{\Psi} - \tilde{\Psi}_c + O(|\tilde{\Psi} - \tilde{\Psi}_c|^{1+\beta}), \quad H^{-1}(\tilde{\mathbf{x}}) = \tilde{\mathbf{x}} + \tilde{\Psi}_c + O(|\tilde{\mathbf{x}}|^{1+\beta}) \tag{A.34}$$

for some constant $\beta \in (0, 1)$.

Proof. This is a corollary of Theorem 7.1 in [38]. Without loss of generality, we assume $\tilde{\Psi}_c = 0$. Otherwise we can define a shift $S : \mathcal{U} \rightarrow \mathbb{R}^{2d}$, $S(\tilde{\Psi}) = \tilde{\Psi} - \tilde{\Psi}_c$. Since $\tilde{\Psi}_c$ is invariant under T^t , we have $ST^tS^{-1}(0) = 0$. We can consider the homeomorphism $\tilde{H} = HS$.

We first consider the 1-time solution T^1 . By Theorem 7.1 in [38], there is a homeomorphism H_0 which satisfies $H_0(0) = 0$, $H_0T^1 = L^1H_0$ and

$$H_0(\tilde{\mathbf{x}}) = \tilde{\mathbf{x}} + O(|\tilde{\mathbf{x}}|^{1+\beta}), \quad H_0^{-1}(\tilde{\mathbf{x}}) = \tilde{\mathbf{x}} + O(|\tilde{\mathbf{x}}|^{1+\beta}).$$

Then we define

$$H = \int_0^1 L^{-s}H_0T^s \, ds. \tag{A.35}$$

We first verify $HT^t = L^tH$ for any $t > 0$. Indeed,

$$L^tH = \int_0^1 L^{t-s}H_0T^{s-t} \, dsT^t = \left(\int_{-t}^0 + \int_0^{1-t} \right) L^{-s}H_0T^s \, dsT^t.$$

Since $H_0 = L^{-1}H_0T$, the first term is

$$\int_{-t}^0 L^{-s}H_0T^s \, dt = \int_{-t}^0 L^{-s-1}H_0T^{s+1} \, ds = \int_{1-t}^1 L^{-s}H_0T^s \, ds.$$

So we obtain

$$L^tH = \int_0^1 L^{-s}H_0T^s \, dsT^t = HT^t.$$

To show that H also satisfies condition (A.34), we utilize Taylor expansion in a neighborhood of $\tilde{\Psi}_c$

$$T^s\tilde{\mathbf{x}} = \nabla T^s(\tilde{\Psi}_c)\tilde{\mathbf{x}} + O(|\tilde{\mathbf{x}}|^2).$$

Note that $T^t(\tilde{\mathbf{x}})$ is the solution of (A.6), we have

$$\frac{d}{dt}\nabla T^t(\tilde{\mathbf{x}}) = \nabla \frac{dT^t}{dt} = \nabla \begin{bmatrix} \Psi_2 \\ -\nabla U(\Psi_1) \end{bmatrix} = \begin{bmatrix} 0 & I \\ -\nabla U(\Psi_1) & 0 \end{bmatrix} \nabla T^t(\tilde{\mathbf{x}}).$$

Taking $\tilde{\mathbf{x}} = \tilde{\Psi}_c$, we obtain

$$\frac{d}{dt}\nabla T^t(\tilde{\Psi}_c) = J\nabla T^t(\tilde{\Psi}_c),$$

where

$$J = \begin{bmatrix} 0 & I \\ A^2 & 0 \end{bmatrix}.$$

Based on the fact $T^t(\tilde{\Psi}_c) = \tilde{\Psi}_c$, we get $\nabla T^t(\tilde{\Psi}_c) = e^{Jt}$ and

$$T^s\tilde{\mathbf{x}} = e^{Js}\tilde{\mathbf{x}} + O(|\tilde{\mathbf{x}}|^2).$$

We obtain

$$H_0T^s\tilde{\mathbf{x}} = T^s\tilde{\mathbf{x}} + O(|T^s\tilde{\mathbf{x}}|^{1+\beta}) = e^{Js}\tilde{\mathbf{x}} + O(|\tilde{\mathbf{x}}|^{1+\beta}).$$

Substituting the above into (A.35) and note that $L^s = e^{Js}$, we get

$$H = \int_0^1 L^{-s}H_0T^s \, ds = \tilde{\mathbf{x}} + O(|\tilde{\mathbf{x}}|^{1+\beta}).$$

We now turn to H^{-1} . We can check that

$$H^{-1} = \int_0^1 T^{-s} H_0^{-1} L^s ds. \quad (\text{A.36})$$

From (A.35) we obtain

$$H \int_0^1 T^{-s} H_0^{-1} L^s ds = \int_0^1 \int_0^1 L^{-t} H_0 T^{t-s} H_0^{-1} L^s dt ds.$$

(A.36) follows by noting that $L^{t-s} = H_0 T^{t-s} H_0^{-1}$. Similar procedure can be applied to get the estimate $H^{-1}(\tilde{\mathbf{x}}) = \tilde{\mathbf{x}} + O(|\tilde{\mathbf{x}}|^{1+\beta})$. \square

Lemma A.6. *Let \mathcal{U} be the neighborhood of $\tilde{\Psi}_c$ ensured by Lemma A.5. Then*

$$\int_0^T \sqrt{\Theta_T(t)} dt \quad (\text{A.37})$$

is uniformly bounded with respect to T for any initial $\mathbf{x}_s \in \partial\mathcal{U}$ and terminal $\mathbf{x}_f \in \partial\mathcal{U}$.

Proof. By Lemma A.2, we only need to consider the case $T \rightarrow +\infty$. Since ψ_T is uniformly bounded, for any finite t_0 , $|\dot{\psi}_T|$ has a positive lower bound and thus

$$\lim_{T \rightarrow \infty} \int_0^{t_0} \sqrt{\Theta_T(t)} dt \leq C.$$

So we will only consider the case when T and t are both sufficiently large.

In the neighborhood \mathcal{U} , we can estimate $\Theta_T(t)$ using the linearized version $\Theta_T^L(t)$. By Lemma A.5, there exists $\beta \in (0, 1)$ such that

$$\begin{aligned} \Psi_1 &= \mathbf{x}_1 + \mathbf{x}_c + O(r^{1+2\beta}), \\ \Psi_2 &= \mathbf{x}_2 + O(r^{1+2\beta}), \end{aligned}$$

where $r = \sqrt{|\mathbf{x}_1|^2 + |\mathbf{x}_2|^2}$. A direct calculation shows

$$\sqrt{\Theta_T(t)} = \frac{\sqrt{F(t) + G_1(t)}}{|\mathbf{x}_2|^2 + G_2(t)}.$$

The functions $G_1 = O(r^{4+2\beta})$, $G_2 = O(r^{2+2\beta})$. As in the proof of Lemma A.4, we first consider the interval $[0, T/2]$. r^2 can be explicitly written as

$$\begin{aligned} r^2 &= \sum_{i \in S} (1 - e^{-2\mu_i T})^{-2} [(p_i e^{\mu_i(2t-T)} + q_i)^2 + \mu_i^2 (p_i e^{\mu_i(2t-T)} - q_i)^2] e^{-2\mu_i t} \\ &\quad + \sum_{i \in \bar{S}} (1 - e^{-2\mu_i T})^{-2} [(1 - e^{-2\mu_i t})^2 + \mu_i^2 (1 + e^{-2\mu_i t})^2] e^{2\mu_i(t-T)}. \end{aligned}$$

Note that the coefficients of $e^{-2\mu_i t}$ and $e^{2\mu_i(t-T)}$ can not be zero, so there are constants $c > 0, C > 0$ such that

$$c \left(\sum_{i \in S} e^{-2\mu_i t} + \sum_{i \in \bar{S}} e^{2\mu_i(t-T)} \right) \leq r^2 \leq C \left(\sum_{i \in S} e^{-2\mu_i t} + \sum_{i \in \bar{S}} e^{2\mu_i(t-T)} \right).$$

If we denote $m = \min S$, $n = \min \bar{S}$, we have

$$c(e^{-2\mu_m t} + e^{2\mu_n(t-T)}) \leq r^2 \leq C(e^{-2\mu_m t} + e^{2\mu_n(t-T)}) \quad (\text{A.38})$$

when t is sufficiently large.

Recall that

$$\begin{aligned} |\mathbf{x}_2|^2 &= \sum_{i \in S} \mu_i^2 (1 - e^{-2\mu_i T})^{-2} [p_i e^{\mu_i(2t-T)} - q_i]^2 e^{-2\mu_i t} \\ &\quad + \sum_{i \in \bar{S}} \mu_i^2 (1 - e^{-2\mu_i T})^{-2} [1 + e^{-2\mu_i t}]^2 e^{2\mu_i(t-T)}. \end{aligned}$$

Case 1: $\mu_m > \mu_n$. Let

$$t_c = \frac{\mu_n T}{\mu_n + \mu_m} < \frac{T}{2}.$$

It is easy to check that $[p_i e^{\mu_i(2t-T)} - q_i]^2$ has a positive lower bound when $t < t_c$. In $[0, t_c]$, $e^{-2\mu_m t} \geq e^{2\mu_n(t-T)}$. So we have

$$r^{2(1+\beta)} \leq C e^{-2(1+\beta)\mu_m t} \leq C e^{-2\mu_m t} \leq \frac{1}{2} |\mathbf{x}_2|^2$$

when t is sufficiently large. In $[t_c, T/2]$, $e^{-2\mu_m t} \leq e^{2\mu_n(t-T)}$. Since $T - t \geq T/2$, we have

$$r^{2(1+\beta)} \leq C e^{2(1+\beta)\mu_n(t-T)} \leq C e^{2\mu_n(t-T)} \leq \frac{1}{2} |\mathbf{x}_2|^2$$

when T is large enough. Thus we obtain $|G_2| \leq \frac{1}{2} |\mathbf{x}_2|^2$, which yields

$$\begin{aligned} \int_0^{T/2} \sqrt{\Theta_T(t)} dt &\leq C \int_0^{T/2} \frac{\sqrt{F}}{|\mathbf{x}_2|^2} + \frac{\sqrt{|G_1|}}{|\mathbf{x}_2|^2} dt \\ &\leq C \int_0^{T/2} \sqrt{\Theta_T^L(t)} dt + C \int_0^{t_c} e^{-2\mu_m(1+\beta)t+2\mu_m t} dt \\ &\quad + C \int_{t_c}^{T/2} e^{2\mu_n(1+\beta)(t-T)-2\mu_m(t-T)} dt \\ &\leq C \int_0^{T/2} \sqrt{\Theta_T^L(t)} dt + \frac{C}{2\beta\mu_m} + \frac{C}{2\beta\mu_n}. \end{aligned} \tag{A.39}$$

By Lemma A.4, we obtain that $\int_0^{T/2} \sqrt{\Theta_T(t)} dt$ is uniformly bounded.

Case 2: $\mu_m \leq \mu_n$. We have $e^{-2\mu_m t} \geq e^{2\mu_n(t-T)}$. Eq. (A.38) yields $r^2 = O(e^{-2\mu_m t})$. If there exists t_m such that $p_m e^{\mu_m(2t-T)} - q_m = 0$, then in a δ -neighborhood of t_m ,

$$\sqrt{\Theta(t)} \leq \frac{F(t) + O(e^{-\mu_m(1+\beta)T})}{C^2(t - t_m)^2 e^{-\mu_m T} + e^{-\mu_n T} + O(e^{-\mu_m(1+\beta)T})}.$$

Applying similar argument as in the proof of Case 2.1, Lemma A.4, we can show that $\int_{t_m-\delta}^{t_m+\delta} \sqrt{\Theta(t)} dt$ is uniformly bounded. Outside this δ -neighborhood, we have

$$r^{2(1+\beta)} \leq C e^{-2(1+\beta)\mu_m t} \leq C e^{-2\mu_m t} \leq \frac{1}{2} |\mathbf{x}_2|^2$$

for sufficiently large t . So the integration

$$\begin{aligned} \int_0^{T/2} \sqrt{\Theta_T(t)} dt &\leq C \int_0^{T/2} \frac{\sqrt{F}}{|\mathbf{x}_2|^2} + \frac{\sqrt{G_1}}{|\mathbf{x}_2|^2} dt \\ &\leq C \int_0^{T/2} \sqrt{\Theta_T^L(t)} dt + C \int_{t_m-\delta}^{t_m+\delta} + C \int_0^{T/2} e^{-2\mu_m(1+\beta)t+2\mu_m t} dt \\ &\leq C \int_0^{T/2} \sqrt{\Theta_T^L(t)} dt + C + \frac{C}{2\beta\mu_m} \end{aligned}$$

is also uniformly bounded.

In all, we have shown that $\int_0^{T/2} \sqrt{\Theta_T(t)} dt$ is uniformly bounded. Similar argument applies to $\int_{T/2}^T \sqrt{\Theta_T(t)} dt$. \square

Lemma A.6 shows that in a neighborhood of critical point \mathbf{x}_c , φ'_k has uniformly bounded variation.

Lemma A.7. *Suppose that the graph limit φ^* passes through a critical point \mathbf{x}_c at α_c . Then there is an interval $[\alpha_-, \alpha_+]$ which contains α_c such that $\{\varphi'_k(\alpha)\}$ has uniformly bounded variation in this interval.*

Proof. Denote $\mathcal{U} = \{\mathbf{x} \mid |\mathbf{x} - \mathbf{x}_c| < 2\delta\}$ in which Lemma A.6 holds, and $\mathcal{V} = \{\mathbf{x} \mid |\mathbf{x} - \mathbf{x}_c| < \delta\} \subset \mathcal{U}$. Define (α_-, α_+) to be an interval satisfying the following two conditions: (1) $\alpha_c \in (\alpha_-, \alpha_+)$; (2) $\forall \alpha \in (\alpha_-, \alpha_+)$, $\varphi^*(\alpha) \in \mathcal{V}$; (3) $\alpha_+ - \alpha_- > 0$. Since φ_k uniformly converges to φ^* , when k is sufficiently large,

$$|\varphi_k(\alpha) - \mathbf{x}_c| \leq |\varphi_k(\alpha) - \varphi^*(\alpha)| + |\varphi^*(\alpha) - \mathbf{x}_c| < 2\delta, \quad \alpha \in (\alpha_-, \alpha_+).$$

Denote $I = [\alpha_-, \alpha_+]$, we have $\varphi_k(\alpha) \in \mathcal{U}$ for any $\alpha \in I$ when k is sufficiently large.

The total variation of φ'_k in I is

$$\bigvee_{\alpha_-}^{\alpha_+} \varphi'_k = \sup_{\Delta} \sum_{j=1}^n |\varphi'_k(\alpha_{j+1}) - \varphi'_k(\alpha_j)|, \quad (\text{A.40})$$

where Δ is a partition of I such that

$$\alpha_- = \alpha_0 < \alpha_1 < \alpha_2 \cdots < \alpha_{n+1} = \alpha_+.$$

If for any k , $E_k > U(\varphi_k(\alpha))$ for $\alpha \in I$, then $\varphi_k \in C^2(I)$. The total variation in this interval can be estimated by

$$\bigvee_{\alpha_-}^{\alpha_+} \varphi'_k \leq \int_{\alpha_-}^{\alpha_+} |\varphi''_k| \, d\alpha.$$

By Lemma A.6, it is uniformly bounded.

If $U(\varphi_k(\alpha)) = E_k$ holds for some α , by Lemma A.1, these points are finite. As in Lemma A.3, we denote the elements of $\{\alpha \mid U(\varphi_k(\alpha)) = E_k\}$ by $\alpha_1^k < \alpha_2^k < \cdots < \alpha_N^k$, and divide the summation in (A.40) into two cases. For Case I, we have

$$\sum_{j \in \text{I}} |\varphi'_k(\alpha_{j+1}) - \varphi'_k(\alpha_j)| \leq 2MN.$$

For Case II, we have

$$\sum_{j \in \text{II}} |\varphi'_k(\alpha_{j+1}) - \varphi'_k(\alpha_j)| \leq \sum_{l=1}^N \int_{\alpha_l^k}^{\alpha_{l+1}^k} |\varphi''_k| \, d\alpha \leq \int_0^{T_k} \sqrt{\Theta_k(t)} \, dt$$

by noting the fact $\varphi_k \in C^2(\alpha_l^k, \alpha_{l+1}^k)$. It is also uniformly bounded by Lemma A.6. \square

Proof of Proposition 3.11. By Assumption 2.5, the number of critical points are finite. Without loss of generality, we assume that φ^* passes through only one critical point \mathbf{x}_c at $\alpha = \alpha_c$. We will show that every component of φ'_k is uniformly bounded and has uniformly bounded variation. Denote $\varphi_k^{(i)}$ the i th component of φ'_k . $|\varphi_k^{(i)}| \leq |\varphi'_k| \leq M$ trivially holds.

By Lemma A.7, there is an interval $I = (\alpha_-, \alpha_+)$ which contains α_c such that $\{\varphi'_k\}$ has uniformly bounded variation in I . Outside the interval I , the function $E^* - U(\varphi^*(\alpha)) > 2m > 0$ for some positive constant m since $E^* = \max U(\mathbf{x})$. From the fact that $\varphi_k \rightarrow \varphi^*$ uniformly, we obtain $E_k - U(\varphi_k) > m$ for any $\alpha \in [0, 1] \setminus (\alpha_-, \alpha_+)$ when k is large enough. This implies $\varphi_k \in C^2([0, 1] \setminus I)$. The total variation of φ'_k on $[0, 1] \setminus I$ can be bounded by

$$\bigvee_{[0,1] \setminus I} \varphi'_k = \int_{[0,1] \setminus I} |\varphi''_k| \, d\alpha = \int_{[0,1] \setminus I} \frac{|\varphi'_k| \sqrt{|\nabla U|^2 |\varphi'_k|^2 - \langle \nabla U, \varphi'_k \rangle^2}}{2E_k - 2U(\varphi_k)} \, d\alpha \leq \frac{M_U M^2}{m},$$

where M_U is the upper bound of $|\nabla U(\varphi_k)|$. This shows that the sequence $\{\varphi_k\}$ has uniformly bounded variation.

With Helly's theorem, we can choose subsequence $\{\varphi'_{k_l}\}$ such that φ'_{k_l} converges almost everywhere to some function g with $|g(\alpha)| \leq M$ and bounded variation. By applying the dominated convergence theorem to

$$\varphi_{k_l}(\alpha) = \mathbf{x}_s + \int_0^\alpha \varphi'_{k_l}(\beta) \, d\beta,$$

we get

$$\varphi^*(\alpha) = \lim_{l \rightarrow \infty} \varphi_{k_l}(\alpha) = \mathbf{x}_s + \lim_{l \rightarrow \infty} \int_0^\alpha \varphi'_{k_l}(\alpha) d\alpha = \mathbf{x}_s + \int_0^\alpha g(\beta) d\beta.$$

So $g(\alpha) = \varphi^{*'}(\alpha)$ almost everywhere. The proof is done.